J. Phys. II France 4 (1994) 377-404 FEBRUARY 1994, PAGE 377

Classification
Physics Abstracts
61.30 — 64.60 — 64.70

Nucleation of focal conic domains in smectic A liquid crystals

O. D. Lavrentovich ([1, *]), M. Kléman ([2, 3]) and V. M. Pergamenshchik ([4,*])

([1]) Liquid Crystal Institute and Department of Physics, Kent State University, Kent, 44242 Ohio, U.S.A.
([2]) Laboratoire de Physique des Solides, Université de Paris-Sud, 91405 Orsay Cedex, France
([3]) Laboratoire de Minéralogie-Cristallographie, Universités Pierre et Marie Curie et Paris VII, 4 Place Jussieu, 75252 Paris Cedex 05, France
([4]) Faculty of Mathematical Sciences, University of Southampton, Southampton, SO9 5NH, U.K.

(*Received 25 May 1993, received in final form 19 October 1993, accepted 22 October 1993*)

Abstract. — The first-order structural transitions caused by an external magnetic field or by a surface anchoring are considered for a smectic A liquid crystal in the restricted geometry of a flat cell. The transition occurs by nucleation of focal conic domains. The free energy of the system is calculated as a function of the order parameter ρ = domain radius/cell thickness for finite value of the splay (K) and a saddle-splay ($\bar{K}$) elastic constants and the anchoring coefficient. For small ρ the behavior of the system is defined by the balance of the stabilising elastic term and destabilising field (or anchoring) term. Homogeneous nucleation from ideal uniform state is hindered by high energetic barrier unless $\bar{K}$ is positive and comparable (or larger) than K. A few possible scenarios of heterogeneous nucleation have been considered, among them the nucleation at local layer undulations and the nucleation at field-induced dislocations. The most effective and general scenario is the nucleation at distortions (dislocations) caused by bulk or surface irregularities. The expansion of the domain ($\rho \gg 1$) is governed by the balance between the field and surface anchoring and does not depend directly on the elastic constants. The saturation field that provides the domain expansion can be smaller than the threshold field for other known mechanisms of the SmA instabilities.

1. Introduction.

The equilibrium structure of layered liquid crystals, such as the smectic A (SmA), consists of a stack of flat parallel layers. The rodlike molecules of each SmA layer orient in the direction normal to the layers. To change the layer thickness usually requires energies considerably greater than needed to curve the layers [1, 2]. Similar properties appear in lyotropic lamellar phases composed of surfactant layers and in cholesteric liquid crystals with a helical pitch much smaller than the characteristic curvatures of the structure.

(*) Also with the Institute of Physics, Academy of Science, Kyïv, Ukraine.

If the layered liquid crystal such as SmA is located in a boundered volume or undergoes an action of an external field, a contradiction arises between the condition of the constant layer thickness and an external orientation force. Typically these frustrations relax through one-dimensional rather than two-dimensional defects. The singularities have a special shape (e.g., conjugated pairs of ellipse and hyperbola) and serve as a frame of the focal conic domain (FCD). Within the FCD the SmA is curved in such a manner that the layer thickness is equal to the equilibrium value everywhere except along the vicinity of two conjugated lines. In the simplest case of the torical FCD (TFCD) the defect pair is represented by a circle and a straight line passing through the center of the circle. The region of deformations is restricted by the circular cylinder. It is remarkable that the layers are perpendicular to the cylinder surface. Thus the TFCD can be smoothly embedded into the matrix of parallel layers. The reason for its appearance can be the tendency of the substrate or an external field to orient the layers normally to the substrate : this orientation is brought about by the TFCD structure in the base region (Fig. 1).

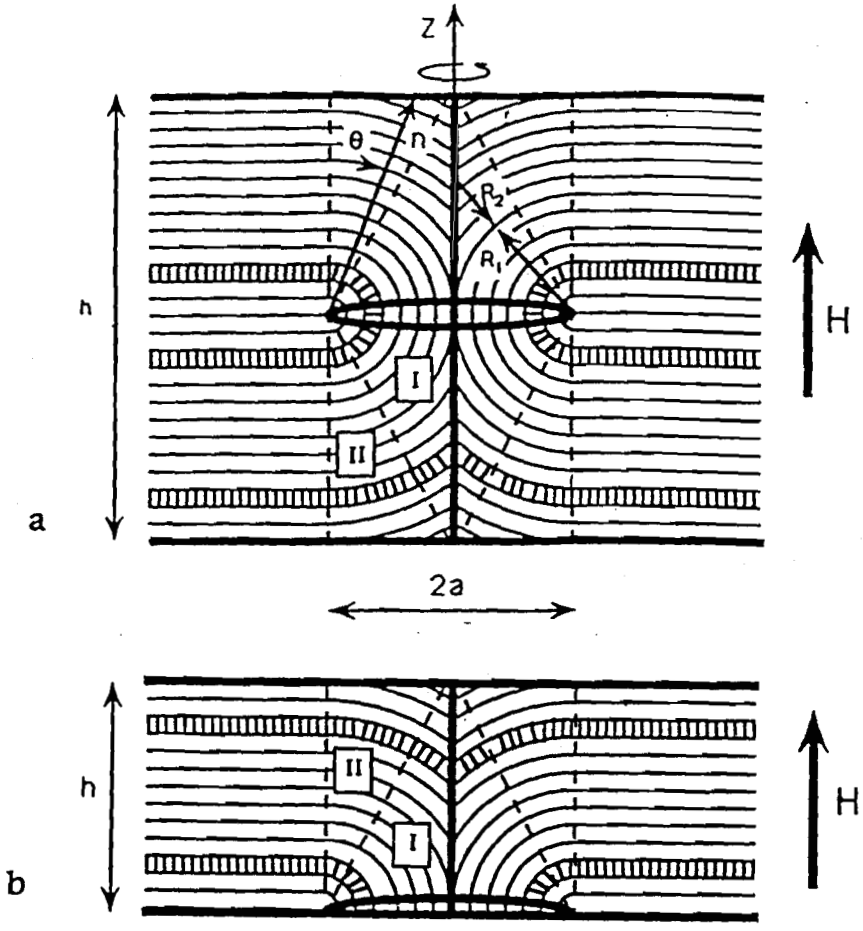

Fig. 1. — Torical focal conic domain (TFCD) with base located at the middle plane of the cell (a) or at the surface of the cell (b). The smectic layers are folded around circle ; this circle as well as the line of rotation symmetry are two linear defects in the director distribution. The domain is smoothly embedded into the matrix composed of flat horizontal layers. In the central part of the domain the layers are reoriented by angle $\pi/2$ in comparison with the outside layers. The region of deformations is restricted by the cylindrical surface with radius a.

When the FCD appears in a sample as a result of competition between bulk curvatures and boundary conditions, it turns out that the radius a of the stable FCD has to be larger than some critical value a_{crit} [3, 4]. This critical radius is defined roughly as [3, 4]

$$a_{crit} \sim K/|\Delta\sigma|\,,$$

where K is a splay elastic constant and $\Delta\sigma$ is a surface tension anisotropy. Typically the critical size is macroscopic (0.1-10 μm). The smaller FCD are unstable because the curvature of layers is too large to be compensated by the surface energy gain.

Numerous experiments (see, e.g., recent ones [3-8] and review [9]) show the possibility of *transitions* between a domain-free state ($a = 0$) and focal conic textures composed of FCD with macroscopic size ($a > a_{crit}$). The mechanism of the « tunneling » of these macroscopic defects through the region of instability ($0 < a < a_{crit}$) is unclear. The problem is similar to that considered for the field induced first-order point-ring defect transition in nematic droplets that also looks formally like an under-barrier tunneling [10].

Experiments [3-8] which clearly show the occurrence of macroscopic TFCDs from « nothing » motivated us to discuss the nucleation of these objects. Our consideration is restricted to the most popular and important (because of possible applications) geometry of a flat smectic A cell of finite thickness where the TFCDs occur due to the action of the external field or the anisotropy in the surface tension. The thermal generation of TFCD's from the supercooled nematic or isotropic phase has been observed experimentally and treated using semiempirical heterogeneous nucleation theory by Chou *et al.* [11]. This process is defined by cooling rate and the temperature of supercooling of high-temperature phase [11]. In our study the TFCDs are supposed to nucleate as a result of field or surface action in the whole temperature region of the SmA phase. The particular case of field-induced bulk nucleation was briefly discussed in reference [12]. We adopt the geometrical approach [13] to describe the TFCD, which implies that the TFCD size is larger than the layer thickness. This approach is justified by the fact that the scale of interest is macroscopic (as defined, e.g., by the ratio $K/|\Delta\sigma|$).

In section 2 we present a geometrical description of the problem and discuss the possible driving forces of the TFCD's nucleation. Section 3 contains general remarks on the scaling behavior of the TFCD's energy while section 4 is devoted to exact calculation of this energy as a function of the domain size, cell thickness and material constants like elastic moduli and surface tension anisotropy. The results of the section 6 allow us to discuss the behavior of the system for two limiting regimes : large « order parameter » ($p \gg 1$) which is chosen as a ratio of the domain radius to the cell thickness, section 5, and small order parameter ($p \ll 1$), section 6. The appearance of the TFCD is the first-order phase transition. The barrier between the uniform and the domain states turns out to be too high to be surmounted by the thermal fluctuations. To explain numerous observations of the TFCD's nucleation we consider different mechanisms that can help to overcome the difficulty : the Parodi's dislocation instability (Sect. 7), the Helfrich-Hurault undulation instability (Sect. 8) and the heterogeneous nucleation at the bulk or surface irregularities of the cell (Sect. 9).

2. Geometry of TFCD.

The system under consideration is a flat sample of thickness h restricted by two horizontal rigid plates. In the initial state the smectic layers are oriented parallel to the plates and the director $\mathbf{n}$ is oriented vertically. This orientation can be achieved either (a) by special (homeotropic) treatment of the plates or (b) by a magnetic ($\mathbf{H}$) or electric ($\mathbf{E}$) field applied along the vertical axis Z, if the preferable surface orientation is tangential but the SmA possesses positive diamagnetic ($\Delta\chi$) or dielectric ($\Delta\varepsilon$) anisotropy. The situations (a) and (b) differ in the driving

force of the TFCD appearance. In the (a) case the TFCDs are caused by the action of the vertical field when $\Delta\chi < 0$ (or $\Delta\varepsilon < 0$). It is a *field-driven transition*. The second scenario is an *anchoring-driven transition* between the field-oriented homeotropic state and the TFCD state which occurs when the surface tension coefficient for tangential orientation ($\sigma_\parallel$) of molecules is smaller than the corresponding coefficient for the tilted or homeotropic ($\sigma_\perp$) orientation ($\Delta\sigma = \sigma_\parallel - \sigma_\perp < 0$) and when the applied field is reduced.

Both scenarios of nucleation imply the appearance and growth of the TFCD embedded in the matrix of horizontally oriented layers. In principle, the circular base of the TFCD can nucleate at the plate *surface* or in the *bulk* of the system or even *outside* the sample. The last geometry of a « virtual » circle was suggested by Steers *et al.* [14] and developed by Fournier [15] for SmA film placed in between two isotropic media. This situation deserves separate consideration, but here we will restrict ourselves to surface and bulk nucleation, in accordance with the experimental observations available [3-8, 16].

Let us consider an analytical description of TFCD following Kléman's model [13]. The smectic layers are distorted inside a cylindrical volume with radius a and height h. The two principal radii of curvature, R_1 and height h. The two principal radii of curvature, R_1 and R_2 are different in sign :

$$R_1 = r > 0\,; \quad R_2 = r - a/\sin\theta < 0\,; \tag{1}$$

here r is measured along **n** and varies in the range $[0, r_{max}]$; θ is an angle between the axis Z and **n**, varying in the range $[0, \pi/2]$ (Fig. 1). To complete the description of the axially symmetric TFCD, one should introduce also the azimuthal angular parameter ϕ, $0 \leq \phi \leq 2\pi$, and the infinitesimal area of the layer in coordinates (θ, ϕ) :

$$dS = r(a - r\sin\theta)\,d\theta\,d\phi\,.$$

3. Energy of TFCD : general remarks.

The free energy density of the smectic A subjected to a magnetic field **H** should contain elastic, magnetic and surface terms. The elastic energy per unit volume reads as [1, 2]

$$f_{el} = \frac{K}{2}\left(\frac{1}{R_1} + \frac{1}{R_2}\right)^2 + \bar{K}\frac{1}{R_1 R_2} + \frac{1}{2}B\delta^2, \tag{2}$$

where the first term is associated with the mean curvature of the layers and the second with the Gaussian curvature, possessing modules K and $\bar{K}$, respectively. The second saddle-splay term has to be considered in any modification of the structure that involves a change in the topology of the layers. Such is the case with TFCD nucleation, which requires the appearance of a negative Gaussian curvature [16]. The third term deals with dilation of layers : B is a compression modulus that describes the elastic resistance to changes δ in the layers thickness d.

Elastic constants in (2) are related, $B \sim K/\lambda^2$, where λ is a characteristic length ; $\lambda \sim d$ ($d \sim 30$ Å) far from the SmA-nematic transition. As a result, the curvatures with energy $\sim KL$ are preferable than dilation ($\sim BL^3$) for macroscopic lengths L. Therefore the geometry of TFCD, where the layers remain equidistant by definition ($\delta = 0$ everywhere except two lines), seems especially appropriate to be responsible for structural transformations.

The density of diamagnetic coupling energy is [1, 2]

$$f_f = -\frac{1}{2}\Delta\chi(\mathbf{nH})^2, \tag{3}$$

and can be replaced by a similar expression for dielectric effect.

TFCD violates the homeotropic orientation at the cell plates (Fig. 1) ; thus the surface term f_s that depends on the polar angle θ should be taken into account. The question of the specific form of the function $f_s(\theta)$ is one of the key questions in the physics of liquid crystals that remains unsolved even for a nematic phase.

The simplest form that describes the behavior of the surface energy of the nematic in the vicinity of the equilibrium orientation θ_0, has been proposed by Rapini and Papoular [17] :

$$f_s = f_{s0} + \frac{1}{2}W\sin^2\theta\,. \tag{4}$$

Here $W > 0$ is the anchoring coefficient which can be considered as the work needed to rotate the director from equilibrium orientation $\theta = 0$ the actual one θ [17]. For nematics $W \sim (10^{-4} - 10^{-1})$ erg/cm^2, i.e., it is much smaller than the isotropic part f_{s0} of the surface tension, $f_{s0} \sim 1\text{-}10^2$ erg/cm^2.

SmA might differ in anchoring properties from the nematic phase because of the layered structure (Fig. 2). Tilted orientation of the SmA requires some kind of « melting » to fill the space in the vicinity of a rigid plate. Figure 2b shows triangular parts of the space that cannot be filled with rigid layers. These triangles can be considered, e.g., as dislocation cores. Two extreme situations can be imagined. In the first case the plate is flat or covered with *rigid* surfactant molecules that keep one or the first few SmA layers in a frozen homeotropic orientation. Then the filling can be provided only by « melting » of the SmA structure. Since the number of layers crossing the boundary is $\sim |\sin\theta|$, one could assume that $f_s \sim W|\sin\theta|$ rather than $f_s \sim W\sin^2\theta$. The value of W in this case can be relatively high, of the order of $(10^{-1} - 10)$ erg/cm^2 [18]. Moreover, f_s can be also a *nonmonotonic* function of θ. The nonmonotonic behavior can be expected, for example, at an absolutely flat surface. Tilted orientations $\theta \neq 0,\ \pi/2$ require the surface « melting » of layers ; in contrast, normal $(\theta = 0)$ and tangential $(\theta = \pi/2)$ orientations do not imply melting and thus can correspond to two minima of $f_s(\theta)$. In this case the anchoring coefficient W describing small deviations from $\theta = 0$ or $\theta = \pi/2$ does not coincide with the surface anisotropy $\Delta\sigma$; one can expect that $W \gg \Delta\sigma$. Another possibility can be brought about by flexible surfactant molecules. If the tails of these molecules adopt different tilted orientations and conformations, they can fill the parts of the space that are not filled with SmA layers. The energetical cost of this filling is defined mainly by the conformational energy of the surfactant molecules and can be significantly

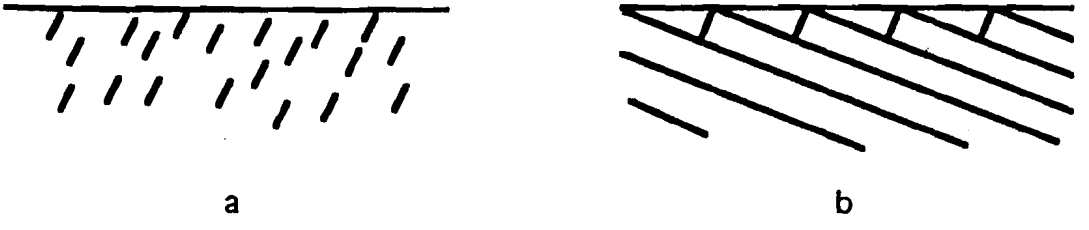

Fig. 2. — Schematic difference in the anchoring for nematic (a) and SmA phase (b). Tilted SmA layers cannot fill the boundary region (triangular parts) perfectly.

smaller than Bd. Moreover, f_s in this case is not obliged to be related to the number of layers and can be close to $\sin^2 \theta$ law. In our calculations we assume the following representation of f_s:

$$f_s = \sigma_\perp + \Delta\sigma \sin^2 \theta ; \quad (5)$$

f_s is minimal for $\theta = 0$ when $\Delta\sigma > 0$ and for $\theta = \pi/2$ when $\Delta\sigma < 0$. Unfortunately, there are only a few experimental estimations of $\Delta\sigma$ for SmA [3-5, 7, 19, 20]. For a SmA-isotropic phase interface $\Delta\sigma \sim 10^{-1}$ erg/cm^2 [7], while for a SmA-water interface $\Delta\sigma \sim 2.5 \times 10^{-2}$ erg/cm^2 [19]. For similar SmA-glycerine interface $\Delta\sigma \sim 10^{-2}$ erg/cm^2 [4], but for the SmA in contact with the glycerine-lecithin mixture $\Delta\sigma \sim 3 \times 10^{-4}$ erg/cm^2 [3]. Hinov [20] has estimated $\Delta\sigma \sim 4 \times 10^{-2}$ erg/cm^2 for SmA at SiO-coated glass plate. In principle, $\Delta\sigma$ can range from low values ($10^{-4} - 10^{-1}$) erg/cm^2 (measured also for nematics) to (1-10) erg/cm^2 [18].

To describe the process of the TFCD appearance and growth one has to calculate the free energy F of the TFCD taking into account the restricted geometry of the cell. The necessity of exact calculations of the energy as a function of the cell thickness can be illustrated by two extreme situations (shown in Fig. 3) for the field-driven bulk nucleation.

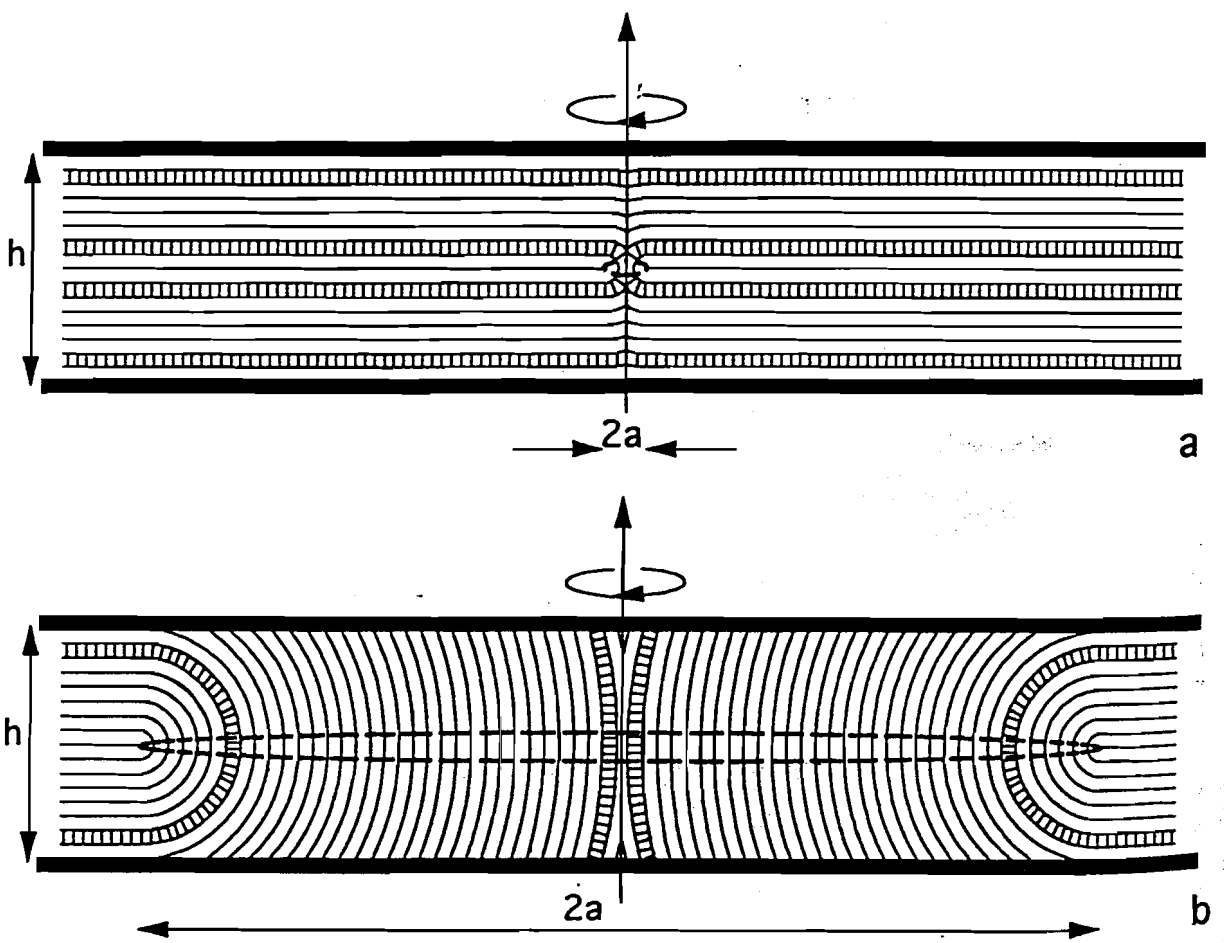

Fig. 3. — The structure of the smectic cell with the torical focal conic domain for two extreme situations: the radius a of the domain is much smaller (a) or much larger (b) than the cell thickness h. The small domain does not change significantly the boundary anchoring : maximal angle of inclination is arctg $(2\,a/h) \ll 1$; the volume of distortion is $\sim a^3$. In contrast, the large domain occupies the volume $\sim ha^2$ and the surface orientation of molecules is practically tangential.

In the first case (Fig. 3a) the domain radius is much smaller than the cell thickness, $a \ll h$. The deformations of layers are restricted by the region of volume a^3 and practically do not change the orientation at the boundaries (at the boundary angle $\theta \sim a/h$ is small). In accordance with equations (2) and (3), the elastic term is $\sim Ka$ and the gain in the magnetic energy is $\sim \Delta\chi\, Ha^3$. Thus the total energy integrated over the volume a^3,

$$F \sim Ka + \Delta\chi\, H^2\, a^3\,, \tag{6}$$

does not depend on the cell thickness in the first approximation.

A completely different situation occurs when $a \gg h$ (Fig. 3b). Now the coupling energy with the field changes the scaling behavior, because the volume of prefered horizontal orientation of molecules is ha^2 rather than a^3. One should consider also the surface term $\Delta\sigma\, a^2$, which is brought about by almost tangential orientation of molecules at the boundaries. The elastic term, however, will be again defined mainly by the radius of the base, $\sim Ka$. Thus the total energy scales as

$$F \sim Ka + \Delta\sigma\, a^2 + \Delta\chi\, H^2\, ha^2\,, \tag{7}$$

and therefore describes a completely different situation in comparison with equation (6). Equation (7) suggests that the growth of the TFCD with $a \gg h$ is defined mainly by the competition of the surface and the field energies. Thus the « saturation » field that provides the unlimited growth of the TFCD and is expected to be measurable in experiments as « homeotropic — to — focal conic domain texture transition threshold », is thickness-dependent, $H_{sat} \sim 1/\sqrt{h}$.

As follows from the consideration given above, to describe the behavior of the focal conic domains one should use proper expressions for their energy as a function of the system size. Unfortunately, up to now the calculations of FCD energy have been restricted by the cases where the system is infinitely large [13] or by special geometry of oily streaks [16]. The determination of F as a function of a, h and other parameters like H and $\Delta\sigma$ is one of the main purposes of this article.

4. Free energy of the defect formation for arbitrary domain radius and cell thickness.

The instability consists in the appearance and growth of the TFCD with variable radius a in the matrix composed by parallel layers. The free energy of the domain formation is expressed as the difference ΔF in the total energy of the defect state $F = (F_e + F_f + F_s)$ and the initial uniform state $F_0 = (F_{e,0} + F_{f,0} + F_{s,0})$. To obtain F and F_0, one should integrate equations (2) and (3) over the domain volume, and (5) over the corresponding surface area. The energy of the uniform initial state of the volume $\pi a^2 h$ is composed of the field and surface contributions :

$$F_0 = -\pi\, \Delta\chi\, H^2\, a^2\, h/2 + 2\,\pi\sigma_\perp\, a^2\,. \tag{8}$$

The finite sample thickness restricts the volume of integration and thus the values of r. It is convenient to subdivide the cylindrical region into a conical volume I and a residual axisymmetrical volume II (Fig. 1). If the TFCD is located at the boundary, then for the region I

$$\xi \leqslant r \leqslant a/\sin\theta - \xi\,, \quad \operatorname{arctg}\,(a/h) \leqslant \theta \leqslant \pi/2\,, \tag{9}$$

while for the region II

$$\xi \leqslant r \leqslant h/\cos\theta\,, \quad 0 \leqslant \theta \leqslant \operatorname{arctg}\,(a/h)\,; \tag{10}$$

here ξ is a cut-off of the elastic energy integration (close to the smectic coherence length).

Conditions (9) and (10) define the core of the circular line as a cylinder with constant radius ξ ; the straight defect line has radius $\sim \xi \sin\theta$ gradually decreasing from ξ to 0 as one moves away along the line from the TFCD's base (Fig. 4). The last assumption is reasonable, because the angle of molecular disorientation in the core of the straight line decreases with distance from the base (Figs. 1, 3 and 4).

The cases of surface nucleation (the circular base of the TFCD is located at the boundary) and bulk nucleation (with base in the middle plane) should be considered separately, because they are accompanied by different behavior of the anchoring term : for example, as shown below, for small domains $(a \ll h)$ $\Delta F_{surf} \propto \Delta\sigma\, a^2$ and $\Delta F_{bulk} \propto \Delta\sigma\, a^4/h^2$.

SURFACE NUCLEATION. — The integration is performed separately for regions I and II, using the conditions (9) and (10). When the TFCD appears, the molecular orientation inclines at the upper surface $[0 \leqslant \theta \leqslant \text{arctg}\ (a/h)]$ and becomes tangential $(\theta = \pi/2)$ at the lower surface. One gets from equations (1-4, 5) the elastic energy of the TFCD in the assumption $a \gg \xi$:

$$F_e = \pi K a \left[\frac{\pi}{2} \ln 2 + L\left(\frac{\pi}{2} - \theta^*\right) + (\pi - 2\theta^*)\left(\ln\frac{a}{\xi} - 2\right) + \right.$$
$$\left. + \theta^* \ln\frac{ah}{\xi\sqrt{a^2+h^2}} - 2\frac{h}{a}\ln\left(1+\frac{a^2}{h^2}\right)\right]$$
$$- \pi\bar{K}h\left[\frac{\pi a}{h} - 2\frac{a}{h}\theta^* + 2\ln\left(1+\frac{a^2}{h^2}\right)\right], \quad (11)$$

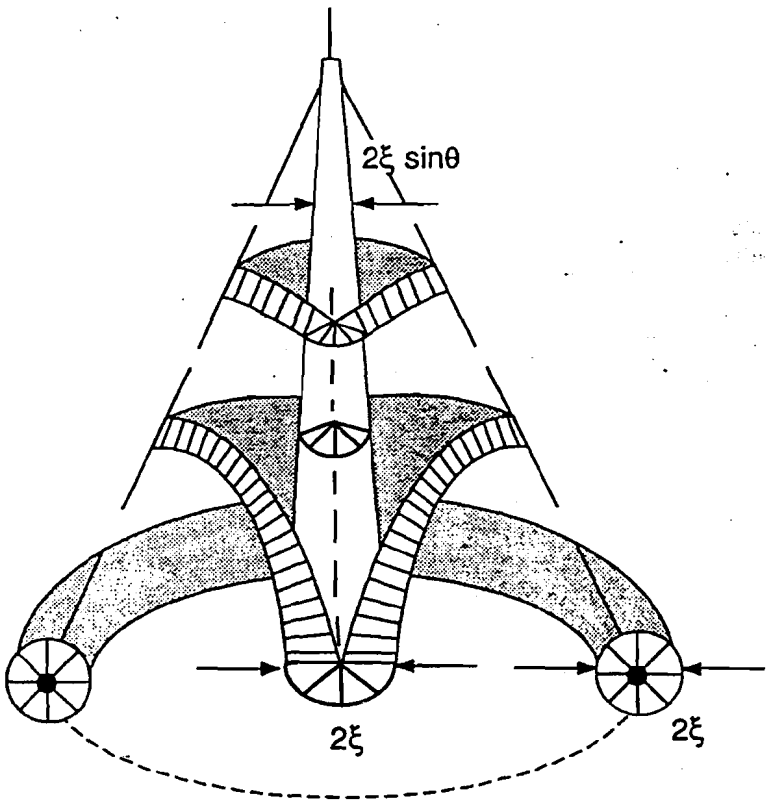

Fig. 4. — The core structure of two defect lines (circle and straight line) that serve as a frame of the torical focal conic domain. The circle has a core of constant thickness $\sim \xi$. The core size of the straight line gradually decreases as one moves away from the domain base because of the decrease of the molecular disorientation in the vicinity of the line.

where $\theta^* = \text{arctg}\,(a/h)$ and $L(x)$ is Lobachevskiy's function [21]

$$L(x) = -\int_0^x \ln \cos t\, dt = x \ln 2 - \frac{1}{2}\sum_{i=1}^{\infty} (-1)^{i-1} \frac{\sin 2ix}{i^2}. \tag{12}$$

With $h \to \infty$, as expected, equation (11) gives results [13, 16] for infinitely large cell thickness.

Equation (11) does not include the core energy of the defect lines as a separate term explicitly ; it cannot be calculated using an elastic approach since the ordering is broken at the core of singularities. As an order of magnitude, the core energy is $\sim K$ per unit length. This circumstance allows one to consider equation (11) as a good approximation to the total elastic energy : the cut-off radius ξ can be chosen to include the core contribution. Moreover, as it will be evident from the discussion in sections 5, 6 and 9, the precise expression for the core energy term is not required for the description of the TFCD nucleation and expansion. In particular, the expansion is defined by the surface area of the TFCD base and terms proportional to the length of singularities are not important.

The surface and field contributions to the TFCD's energy are calculated as :

$$F_s = \pi\, \Delta\sigma \left[2(\sigma_\parallel/\Delta\sigma)\, a^2 - 2\, ah\, \text{arctg}\, \frac{a}{h} + h^2 \ln \left(1 + \frac{a^2}{h^2} \right) \right], \tag{13}$$

and

$$F_f = \frac{\pi}{6} \Delta\chi\, H^2 \left[-a^2 h - 3\, ah^2\, \text{arctg}\, \frac{a}{h} + h^3 \ln \left(1 + \frac{a^2}{h^2} \right) + \frac{\pi}{2} a^3 - a^3\, \text{arctg}\, \frac{a}{h} \right]. \tag{14}$$

Using equations (8), (11-14), the free energy of the surface nucleation, $\Delta F_{SN} = F - F_0 = F_e + F_s + F_f - F_0$ can be expressed as a function of the dimensionless TFCD radius $\rho = a/h$:

$$\Delta F_{SN} = \pi K h \rho \left[\frac{\pi}{2} \ln 2 + L(\text{arcctg}\, \rho) + 2\, \text{arcctg}\, \rho \left(\ln \frac{h\rho}{\xi} - 2 \right) \right.$$

$$\left. + \text{arctg}\, \rho \ln \frac{\rho h}{\xi \sqrt{\rho^2 + 1}} - \frac{2}{\rho} \ln (1 + \rho^2) \right]$$

$$- \pi \bar{K} h [\pi\rho - 2\, \rho\, \text{arctg}\, \rho + 2 \ln (1 + \rho^2)] + \pi h^2 \Delta\sigma\, [2\, \rho^2 - 2\, \rho\, \text{arctg}\, \rho + \ln (1 + \rho^2)]$$

$$+ \frac{\pi}{6} \Delta\chi\, H^2 h^3 \left[2\, \rho^2 - 3\, \rho\, \text{arctg}\, \rho + \ln (1 + \rho^2) + \frac{\pi}{2} \rho^3 - \rho^3\, \text{arctg}\, \rho \right]. \tag{15}$$

The dimensionless radius ρ can be considered as an order parameter of the transition. For initial state $\rho = 0$ and $\Delta F_{SN} = 0$.

BULK NUCLEATION. — The molecules incline symmetrically at both surfaces ($0 \leqslant \theta \leqslant \text{arctg}\, 2\rho$) and the surface energy of the domain formation is

$$\Delta F_{BN,s} = \frac{\pi}{2} h^2 \Delta\sigma\, [4\, \rho^2 - 4\, \rho\, \text{arctg}\, 2\rho + \ln (1 + 4\, \rho^2)]. \tag{16}$$

The field and elastic energies can be found from equations (13), (14), by multiplying the corresponding terms by 2 and making substitutions $\rho \to 2\rho$, $h \to h/2$ (to hold the notation of

the order parameter $\rho = a/h$). Finally, the free energy of the bulk nucleation is :

$$\Delta F_{BN} = 2\,\pi K h \rho \left[\frac{\pi}{2} \ln 2 + L(\text{arcctg } 2\,\rho) + 2\,\text{arcctg } 2\,\rho \left(\ln \frac{h\rho}{\xi} - 2 \right) + \right.$$

$$\left. + \text{arctg } 2\,\rho \ln \frac{\rho h}{\xi \sqrt{4\,\rho^2 + 1}} - \frac{1}{\rho} \ln (1 + 4\,\rho^2) \right] - 2\,\pi \bar{K} h [\pi \rho -$$

$$- 2\,\rho\,\text{arctg } 2\,\rho + \ln (1 + 4\,\rho^2)] + \frac{1}{2}\,\pi h^2\,\Delta\sigma\,[4\,\rho^2 - 4\,\rho\,\text{arctg } 2\,\rho + \ln (1 + 4\,\rho^2)]$$

$$+ \frac{\pi}{24}\,\Delta\chi\,H^2\,h^3 [8\,\rho^2 - 6\,\rho\,\text{arctg } 2\,\rho + \ln (1 + 4\,\rho^2) + 4\,\pi\rho^3 - 8\,\rho^3\,\text{arctg } 2\,\rho]\,. \quad (17)$$

Despite the apparent complexity of equations (15) and (17) for the free energies ΔF_{SN} and ΔF_{BN}, these equations have one evident advantage : they are exact for domains of supramolecular size and allow us to describe the behavior of the system in the whole possible range of the order parameter ρ, i.e., from $\rho > \xi/h \cong 0$ to $\rho \to \infty$. As will be shown, the expanded versions of ΔF_{SN} and ΔF_{BN} are quite simple for both small and large scales. It is convenient to start the discussion with graphic representations.

Figures 5 and 6 show the variations of free energies $\Delta F_{SN}(\rho, H)$ and $\Delta F_{BN}(\rho, H)$ calculated

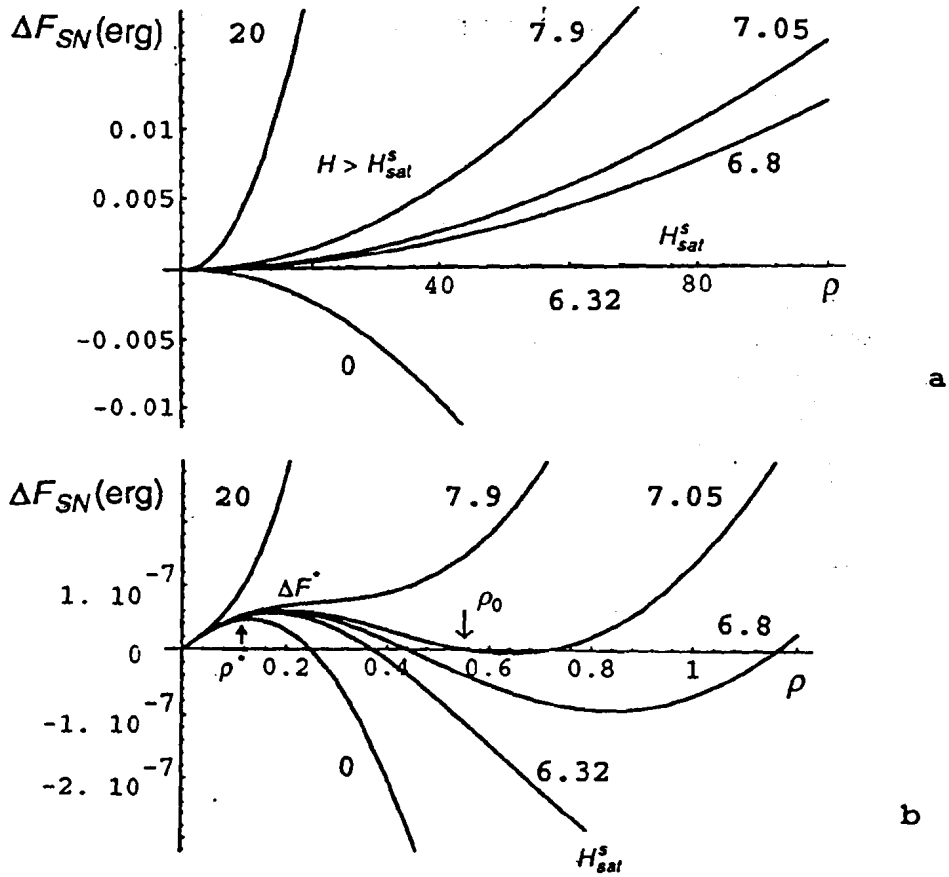

Fig. 5. — Free energy of the torical focal conic domain as a function of the dimensionless radius $\rho = a/h$ for the anchoring-driven nucleation. The domain is supposed to appear at the surface of the cell due to the reorienting action of the surface anchoring when the orienting magnetic field diminishes. Two different scales are shown : large ρ (a) and small ρ (b). Both plots were calculated using the same equation (15) for the same parameters. Different lines correspond to different values of the magnetic field (shown by numbers in kGs units).

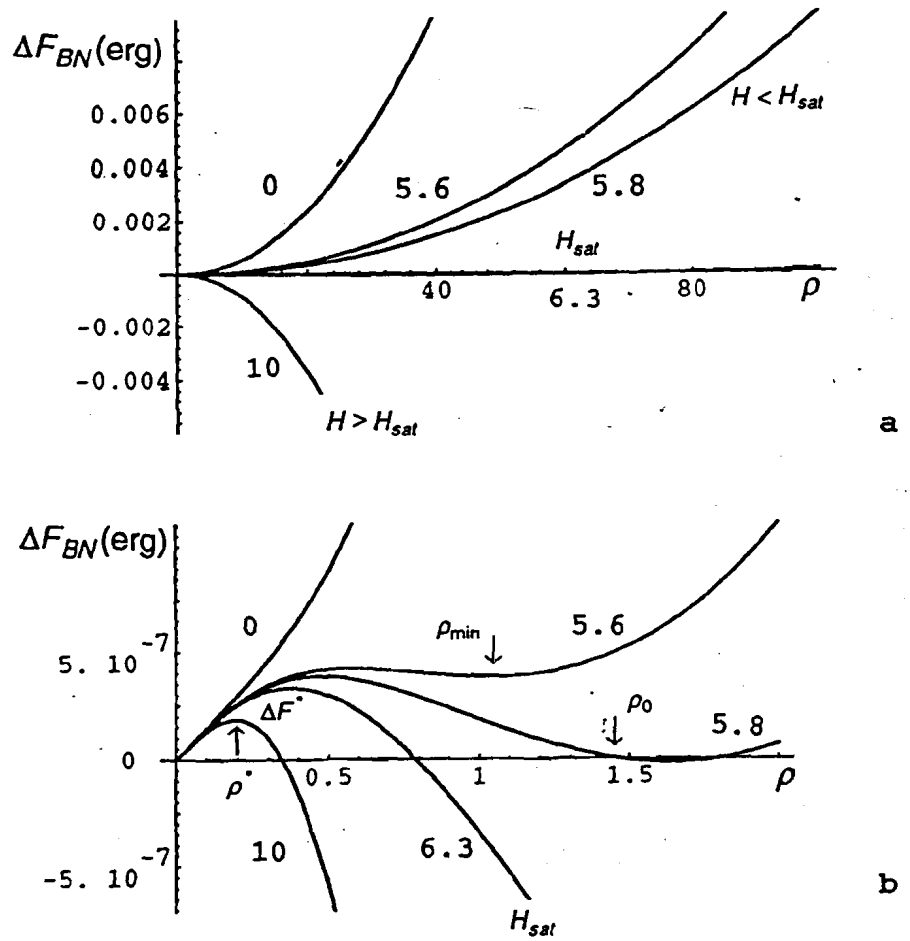

Fig. 6. — Free energy of the torical focal conic domain as a function of the dimensionless radius $\rho = a/h$ for the field-driven nucleation. The domain is supposed to appear in the middle of the cell due to the increasing reorienting action of the field. Two different scales are shown : large ρ (a) and small ρ (b). Both plots were calculated using the same equation (17) for the same parameters. Different lines correspond to different values of the magnetic field (shown by numbers in kGs units).

using equations (15) and (17) with $h = 100$ μm, $K = 10^{-6}$ dyn, $\bar{K} = 0$, $\Delta\chi = 10^{-7}$ CGS and $\Delta\sigma = -10^{-2}$ erg/cm^2 (anchoring-driven surface nucleation, Fig. 5) and $h = 100$ μm, $K = 10^{-6}$ dyn, $\bar{K} = 0$, $\Delta\chi = -10^{-7}$ CGS and $\Delta\sigma = 10^{-2}$ erg/cm^2 (field-driven bulk nucleation, Fig. 6) ; Lobachevskiy's function here and below is calculated with accuracy up to the first 40 terms in equation (12), using « Mathematica. Version 2.1 », Wolfram Research.

The behavior of $\Delta F_{SN}(\rho, H)$ and $\Delta F_{BN}(\rho, H)$ is illustrated for two different scales : large TFCDs (Figs. 5a, 6a) and small TFCDs (Figs. 5b, 6b). It is important to stress that despite seeming differences in the physical picture illustrated by (a) and (b) parts of the figures 5 and 6, *both parts represent the same dependencies* (15) *and* (17) ; the only difference is the scale of pictures.

5. Limit of large FCD.

As already mentioned, the behavior of the free energy differs principally for $\rho \ll 1$ and $\rho \gg 1$, due to the *confined* nature of the system (finite cell thickness). The nucleation of small domains ($\rho \ll 1$) does not mean automatically *the completeness* of the transition, i.e., the ability of the domain to expand significantly (and the opposite is true : the ability to complete

the transition does not imply the possibility of nucleation). The statement is easy to understand using a field-driven transition as an example : for $\rho \ll 1$ the surface anisotropy practically does not hinder the occurrence of the TFCD ; however, the growth of TFCD ($\rho \gg 1$) can be suppressed because the surface term becomes more and more important for growing TFCD. In real experiments the transition between the initial homeotropic state and the final focal-conic domain structure is supposed to be registered when the TFCD is able to expand significantly, i.e., just for the case $\rho \gg 1$. The possible value of the field that provides this large-scale growth is discussed below for the field-driven situation caused by $\Delta\chi < 0$ (Fig. 6).

If the external field H is absent, all molecules are oriented perpendicularly to the plates because of $\Delta\sigma > 0$. ΔF_{BN} has only one minimum at $\rho = 0$ and the initial state is absolutely stable (curve 0 at Fig. 6, where numbers correspond to the value of H expressed in kGs). As H increases the second local minimum appears for some $\rho_{min} \neq 0$ (curves $H = 5.6$ and $H = 5.8$). The uniform state becomes unstable with respect to the formation of the TFCD when $\Delta F_{BN}(\rho_{min}) < 0$. For the moderate field, as expected, the radius of the TFCD can not grow infinitely : the increase of $\rho > \rho_{min}$ is accompanied by the increase of energy (see curve $H = 5.8$) because of the positive surface contribution ($\Delta\sigma > 0$) that becomes important starting with $\rho \sim 1$.

Nevertheless, there is some « saturation » field $H_{BN,\,sat}$, above which the radius of the TFCD grows infinitely. For $H > H_{BN,\,sat}$ the dependency $\Delta F_{BN}(\rho)$ is a negative and monotonically decreasing function for large ρ. In figure 6, $H_{BN,\,sat}$ corresponds to the curve $H = 6.3$ that practically coincides with the axis ρ. To find $H_{BN,sat}$, it is convenient to make a substitution $\rho \to 1/\varepsilon$ in the exact expression (17) for the free energy $\Delta F_{BN}(\rho)$ and expand it in the vicinity of $\varepsilon \to 0$. It yields

$$\Delta F_{BN}(\rho \gg 1) = \left(2\pi\,\Delta\sigma\,h^2 + \frac{\pi}{2}\Delta\chi\,H^2\,h^3\right)\rho^2 + \left(-\pi^2\Delta\sigma\,h^2 - \frac{\pi^2}{8}\Delta\chi\,H^2\,h^3 + hK\pi^2\ln(h/\xi)\right)\rho + \cdots \quad (18)$$

where only the quadratic and linear terms are retained. Since $\rho \gg 1$, equation (18) clearly shows that the decisive is the first (quadratic in ρ) term. Defining $H_{BN,\,sat}$ as a field that makes the first term zero, one finds :

$$H_{BN,\,sat} = 2\sqrt{\frac{\Delta\sigma}{h\,|\Delta\chi|}}. \quad (19)$$

Therefore, the final stage of the TFCD growth depends on *the balance between the field and surface energies* rather than on the elastic energy (including core energy) ; constants K, $\bar{K}$ and B do not enter equation (19). This result is easy to understand, because the central part of a large domain is composed of practically parallel layers that are oriented normally to the cell plates (Fig. 3b). With estimates used above for thermotropic smectics, $H_{BN,\,sat} = 6.3$ kGs. The line $H_{BN,\,sat} = 6.3$ kGs practically coincides with the coordinate axis at figure 6a. The $\Delta F_{BN}(\rho \gg 1)$-dependencies corresponding to $H < H_{BN,\,sat}$ remain positive for large ρ, while for $H > H_{BN,\,sat}$ they are negative and the growth of the domain only decreases the energy.

It is worth noting that $H_{BN,\,sat}$ for modest $\Delta\sigma$ is significally *smaller* than the threshold of two other known instabilities : the Helfrich-Hurault undulation instability [22, 23], which consists in the periodic distortions of layers in the horizontal plane, and Parodi's instability [24], which implies the appearance of the dislocation defects. In both known effects the distortions violate the requirement of constant layer thickness and thus the threshold field is defined by the balance of the field energy and the dilation energy with elastic constant B. For example, for the

Helfrich-Hurault threshold [22, 23] in the geometry with vertical field and $\Delta\chi < 0$ one has an expression (see also Sect. 8, below) :

$$H_{HH} = \sqrt{\frac{2\pi\lambda B}{h|\Delta\chi|}}. \tag{20}$$

One obtains similar expression for Parodi's threshold (see also Ref. [24] and Sect. 7) :

$$H_P = 2\sqrt{\frac{\lambda B}{h|\Delta\chi|}}. \tag{21}$$

Thus the ratios

$$\frac{H_{BN,\,sat}}{H_{HH}} \sim \frac{H_{BN,\,sat}}{H_P} \sim \sqrt{\frac{\Delta\sigma}{\lambda B}} \tag{22}$$

are small, ~ 0.02 (with $\Delta\sigma = 10^{-2}$ erg/cm^2, $\lambda \sim 30$ Å and $B \sim 10^8$ dyn/cm^2). For strongly anchored SmA, the layers are broken in the vicinity of the plates and the anchoring coefficient might be of the order of λB (see Ref. [18]). For this case the ratios (22) are close to unity.

The large-scale behavior of the *anchoring-driven transition* is similar to that described above for the *field-driven bulk nucleation* (Fig. 5). If the field **H** (normal to the cell) is strong enough, all molecules are oriented along **H** (now $\Delta\chi$ is positive) and the equilibrium state is uniform, i.e., ΔF_{SN} has only one minimum at $\rho = 0$. The macroscopic expansion of the TFCD occurs when H is *smaller* than some field $H_{SN,\,sat}$, defined from the condition $\Delta F_{SN}(\rho \gg 1) < 0$. It yields an expression identical to equation (19) with accuracy to the inversion of signs of $\Delta\sigma$ and $\Delta\chi$:

$$H_{SN,\,sat} = 2\sqrt{\frac{|\Delta\sigma|}{\Delta\chi\, h}}, \tag{23}$$

which is not a surprising result, because for large ρ there is no difference in geometry of surface and bulk instabilities (Fig. 3b).

In concluding this section it is important to discuss the specific *range of validity of the large-scale description* used for determination of the saturation fields such as (19) or (23). From the thermodynamical point of view, any response to the external parameter variation means it brings the system into the state with smaller free energy than that in the absence of such response. However, the critical condition for the transition between states 1 and 2 to occur can be written in the form $\Delta F = F(2) - F(1) < 0$ only if 1 transforms into 2 directly without the necessity of increasing the energy. The large-scale pictures (Figs. 5a, 6a) give an impression that this is just the case and the transition between the uniform state (no TFCD) and the state with large TFCD *can* occur directly as an appearance of zero radius domain and its expansion until reaching the macroscopic dimension observed in experiments. In fact, as we will see in the next section, the two states are separated by an *energy barrier* located in the small-scale region, $\rho \ll 1$. As the field becomes higher than $H_{BN,\,sat}$ (field-driven transition) or drops below $H_{SN,\,sat}$ (anchoring-driven transition), the uniform state becomes metastable but the *barrier prevents it from becoming unstable*. Thus actually there are *two* conditions of the transition : first, the condition $\Delta F < 0$, and second, the ability of the system to overcome the barrier between the states. This second condition will be considered below. It is obvious that the real threshold will be determined by the condition that is more difficult to satisfy.

Summarising, the large-scale picture is important to describe the completeness of the transition. It gives correct values of the threshold field if TFCD nuclei somehow have been

created in the system and the only problem is to provide the TFCD with possibility to expand and replace the initial state. However, the large-scale picture does not show the very beginning of the instability, does not show how the TFCD appears from « nothing ». This question should be considered for the small-scale limit, $\rho \ll 1$.

6. Limit of small TFCD.

The free energies (15) and (17) can be expanded for small $\rho \ll 1$:

$$\Delta F = A_1 \rho + A_2 \rho^2 + A_3 \rho^3 + A_4 \rho^4 + \cdots , \tag{24}$$

where the coefficients A_i are different for surface and bulk nucleations and thus will be provided by different indices, SN and BN, respectively. It is easy to check that *the linear term A_1 in both cases is defined solely by the splay and saddle-splay elastic contribution* :

$$A_{SN,1} = \pi^2 Kh(\beta - 2 - \bar{K}/K) , \tag{25}$$

$$A_{BN,1} = 2\,\pi^2 Kh(\beta - 2 - \bar{K}/K) , \tag{26}$$

where $\beta = \ln (2h\rho/\xi) \approx$ Cte. (for $a \gg \xi$ the logarithmic dependence is weak). The anchoring contributes to the second term (but only for a surface-driven effect),

$$A_{SN,2} = \pi\,\Delta\sigma\, h^2 - \pi Kh(3 + \beta - \ln \sqrt{2}) , \tag{27}$$

$$A_{BN,2} = 4\,\pi Kh(\ln \sqrt{2} - \beta - 3) , \tag{28}$$

while the field action defines the cubic terms :

$$A_{SN,3} = \frac{\pi^2}{12} \Delta\chi\, H^2 h^3 , \tag{29}$$

$$A_{BN,3} = \frac{\pi^2}{6} \Delta\chi\, H^2 h^3 . \tag{30}$$

The behavior of the system is determined by the signs and values of the coefficients of expansion. It is natural to assume that in our particular problem (TFCD in the stable SmA phase) the linear coefficient A_1 is always positive, i.e., saddle-splay constant $\bar{K}$ is not too high. Otherwise, even in the absence of the external surface or field torques the layered smectic structure will be unstable with respect to the formation of the TFCDs. In fact, a similar instability occurs during the transition of the lamellar SmA to the anomalous isotropic (sponge) phase where $\bar{K}$ significantly increases [25, 16] and thus can favor the appearance of FCD. We will assume $\bar{K} = 0$. The second coefficient $A_{SN,2}$ depends both on the elastic and surface contributions if the nucleation occurs at the surface. If the tangential orientation of molecules is preferable ($\Delta\sigma < 0$), then $A_{SN,2} < 0$. For homeotropically treated samples with $\Delta\sigma > 0$ the bulk nucleation seems to be more preferable and $\Delta\sigma$ enters only in the fourth term of the expansion. Finally, the third term A_3 is defined solely by the field contribution and can take both positive and negative signs following the sign of $\Delta\chi$.

The dependies $\Delta F(\rho, H)$ for small ρ (Figs. 5b, 6b) clearly demonstrate the first-order character of the transition. $\Delta F(\rho)$ goes through a maximum $\Delta F^* = \Delta F(\rho^*)$ at some critical radius ρ^*, that defines the critical TFCD-nuclei. Only the TFCDs of a sufficiently large radius $\rho > \rho^*$ transform the metastable uniform state into the stable defect state. The TFCDs with $\rho < \rho^*$ (embryos) are unstable and will decay.

The energy barrier that separates the two states is brought about by the positive leading elastic term in the expansion (24). This term scales practically linearly with ρ and this explains why the barrier always exists and is located in the region of relatively small ρ : the driving force, in accordance with equations (27) and (30), contributes only to the *quadratic* (anchoring) or even *cubic* (field) terms.

Despite the fact that for $H \sim H_{sat}$ the uniform state has evidently higher energy than the defect state (Figs. 5, 6), the barrier separating the two states turns out to be too high to allow the transition. Thus the metastable uniform state remains supercooled until H or $\Delta\sigma$ becomes significantly higher than that defined by equations (19) and (23). Similar situations with high potential barriers are known for the problem of bubble nucleation in the electroweak theory, vortex nucleation in superconductors, etc. (see, e.g., Refs. [26] and [27]). Let us consider this question in greater detail for the TFCD.

The application of general nucleation theory (see, e.g., [28]) to the formation of FCD and similar problems, such as nucleation of vortex loops in superfluids or dislocation loops in solids and smectics [29], yields as a basic nucleation rate equation

$$G = G_0 \exp[-\Delta F^*/k_B T], \tag{31}$$

where G is number of nuclei per unit volume and unit time and $G_0 = g_0 n$ is a characteristic rate for microscopic processes, defined by some kinetic coefficient g_0 and by the number n of molecules per unit volume. The kinetic coefficient g_0 is estimated crudely [29] as (sound velocity)/(molecular dimension). Taking the minimal rate of nucleation $G \sim 10^{-1}\,s^{-1}\,cm^{-3}$ and estimates used by Pershan and Prost [29] for thermotropic smectics, $g_0 \sim (10^5\,cm\,s^{-1}/2 \times 10^{-7}\,cm)$ and $n \sim 3 \times 10^{21}\,cm^{-3}$, one finds that the nucleation will be observable if $\Delta F^* \leqslant 80\,k_B T$, or $\Delta F^* \leqslant 3 \times 10^{-12}$ erg. Unfortunately, as shown below, the typical barrier of TFCD nucleation turns out to be higher.

For a qualitative understanding it is sufficient to consider the most favorable situation for the surface-driven transition with the lowest energy barrier ΔF^*_{SN}, when the field is completely removed, $A_{SN,3} = 0$. Then

$$\rho^*_{SN} = -\frac{A_{SN,1}}{2A_{SN,2}} = \frac{\pi K(\beta - 2 - \bar{K}/K)}{2|\Delta\sigma|h + 2K(3 + \beta - \ln\sqrt{2})}, \tag{32}$$

$$\Delta F^*_{SN} = -\frac{A^2_{SN,1}}{4A_{SN,2}}, \tag{33}$$

or, for $|\Delta\sigma|\,h/K \gg 1$ (which is again the most favorable condition),

$$\Delta F^*_{SN} \cong \frac{\pi^3 K^2}{4|\Delta\sigma|}(\beta - 2 - \bar{K}/K)^2. \tag{34}$$

With typical $K = 10^{-6}$ dyn, $\bar{K} = 0$ and $\Delta\sigma = -10^{-2}$ erg/cm^2 one has $\Delta F^*_{SN} \sim 10^{-9}$ erg, i.e., $\Delta F^*_{SN} \gg 80\,k_B T$. The desired $\Delta F^*_{SN} \sim 3 \times 10^{-12}$ erg can be achieved only for systems with $\Delta\sigma$ as high as $\sim (-1)$ erg/cm^2. Of course, nonzero (and positive) $\bar{K}$ can facilitate the nucleation, but up to now high values of $\bar{K}$ have been reported only for lyotropic smectics in the vicinity of the lamellar to anomalous isotropic phase [16].

The same barrier problem appears for field-driven nucleation. We again assume the simplest situation : the field is strong enough, $A_{BN,2}/\sqrt{A_{BN,1}|A_{BN,3}|} = \bar{\omega} \ll 1$. The barrier, located at

$$\rho^*_{BN} \cong \frac{2}{Hh}\sqrt{\frac{K(\beta - 2 - \bar{K}/K)}{|\Delta\chi|}}, \tag{35}$$

is

$$\Delta F^{*}_{BN} \cong \frac{A^{3/2}_{BN,1}}{3\sqrt{3}\,|A_{BN,3}|^{1/2}}(2-\sqrt{3}\,\bar{\omega}+\bar{\omega}^2) \approx \frac{8\,\pi^2 K^{3/2}(\beta-2-\bar{K}/K)^{3/2}}{3\sqrt{|\Delta\chi|}\,H} \tag{36}$$

and remains quite high to be surmounted by fluctuations : $\Delta F^{*}_{BN} \sim 3 \times 10^{-12}$ erg only if the field is as high as $H = H_{barrier} \sim 10^5$ kGs for thermotropics or 200 Gs for ferrosmectics described in [6]. Both estimated fields are much higher than H_{sat}. Here and below $H_{barrier}$ is defined from the condition $\Delta F^{*}/80\,k_B\,T = 1$.

As follows from the consideration given above, the assumption that the field $H \sim H_{sat}$ providing *the expansion* of the TFCD can also *nucleate* the domain from « nothing », is rather exotic one. Nevertheless, the nucleation of FCD is observed experimentally not only in ferrosmectics but also in thermotropic materials for quite modest values of fields or expected $\Delta\sigma$. There are no special reasons to assume that this nucleation in all cases is explained by large $\bar{K}$: at least for thermotropics it is hard to expect that $\bar{K}$ is significantly different from zero. The problem is thus to find the general path of the macroscopic tunneling. An apparent solution of this problem is an assumption that the nucleation starts from a *nonuniform* state rather than from the ideal *uniform* structure considered above. This assumption was used by Chou *et al.* [11], Hinov [4] as well as by Jákli and Saupe [7] to explain experimental findings. Among them is the formation of the TFCDs at the same particular sites of the cell plates, connected probably with local inhomogeneities [11, 7]. In fact (see Ref. [4]), one can find this idea in the article of Friedel [30] : « ... it seems clear also that defects — translation dislocations and focal conics — strongly interfere with the oscillations of the layers, and stabilise the buckled state, in a way that has not been completely elucidated ».

While not pretending to elucidate the question completely, in the remaining part of this article we will consider the possible ways of TFCD generation from the distorted state. In the case of field-induced nucleation the first idea is obvious : to find other mechanisms of distortions and then consider the possibility of TFCD generation by these instabilities for higher values of the driving force. Two types of instabilities of the SmA are known : the Helfrich-Hurault undulations [22, 23] and the Parodi's transition [24]. Both models describe the field instability but do not describe the surface-induced instability. The Helfrich-Hurault effect is a second-order transition : the layer tilt grows continuously from 0 to some finite value when $H \geq H_{HH}$. In contrast, Parodi's effect implies the finite tilt of layers when the field is higher than some critical one which we denote H_P. The tilt is caused by the creation of defects such as dislocation walls. Since this mechanism is formally similar to the nucleation of the TFCD, it will be considered first.

7. Nucleation as a result of Parodi's instability.

Let us briefly reconsider the main features of Parodi's effect [24] and demonstrate that *it is a first-order phase transition* and thus requires special consideration of the *barrier problem.*

As was predicted in reference [24], the field-induced transition occurs as a reorientation of the molecules in the central part of the cell with corresponding appearance of grain boundaries (periodic pattern of disclinations and dislocations) that allow folding of the layers. The defects are located in the vicinity of the plates. The energy of the grain boundary was considered in terms of a continuous density $1/d$ of dislocations with self-energies $\sim K$ (d is the layer's thickness) [24]. The gain in the field energy due to the finite layer tilt θ can be estimated as $F_f \sim \frac{1}{2}\Delta\chi\,H^2\,h\theta^2$ per unit area, while the elastic energy cost of two grain boundaries providing this reorientation is $F_e \sim 2\,K\theta/d$. For the sake of simplicity we will neglect a positive

contribution of the disclination to the total energy. In principle, the saturation field for $\theta \sim 1$ can be found from the condition $F_e + F_f = 0$ which means the equality of the energies of the initial state and the grain-boundary state. It gives

$$H_P = 2\sqrt{\frac{K}{hd|\Delta\chi|}}, \tag{37}$$

which is exactly the threshold field defined by Parodi [24]. The last expression is valid for temperatures far from the SmA-nematic phase transition.

As was shown in section 5, H_P is *higher* than H_{sat} for TFCDs, if $\Delta\sigma < dB$, equation (22). Nevertheless, the physical meaning of H_P is analogous to that of H_{sat} : it defines only the *final stage* of the transition, when θ and the area of the grain boundary are not small. Thus here one has the same problem with the very beginning of the process as in the case of TFCD : for small θ the decisive term is just the positive elastic term and the transition should be hindered by the potential barrier. This barrier is even *infinitely large* when the infinitively long linear dislocations are considered. To provide the finite barrier, one should modify the model and assume that the dislocations nucleate as closed loops with finite radii. Let us consider just one dislocation loop that occurs in the horizontal plane in response to the vertical field.

The elastic energy of an isolated dislocation loop with small radius $r_d \ll \sqrt{\lambda h}$, was estimated as [29, 31] $\sim \pi\lambda B d^2 r_d/\xi$. A gain in the magnetic energy is roughly $\sim \frac{1}{2}\Delta\chi H^2 \theta^2 \times$ (volume of distortions). Here $\theta = d/r_d$; the volume of distortions created by the loop can be estimated taking into account that the penetration length of deformations along the vertical axis is $\sim 2 r_d^2/\lambda$ [1, 2], and the disturbed horizontal area is $\sim \pi r_d^2$. Thus the total energy of the loop is

$$\Delta F_{disl} \sim \pi\lambda B d^2 \frac{r_d}{\xi} + \pi\,\Delta\chi\, H^2 d^2 \frac{r_d^2}{\lambda}, \tag{38}$$

which leads to the critical radius

$$r_d^* = \frac{\lambda^2 B}{2\xi|\Delta\chi| H^2} \tag{39}$$

and the barrier

$$\Delta F^*_{disl} = \frac{\pi\lambda^3 d^2 B^2}{4\xi^2|\Delta\chi| H^2} = \frac{\pi\lambda^2 d^2 K^{1/2} B^{3/2}}{4\xi^2|\Delta\chi| H^2}; \tag{40}$$

(two equivalent representations have been chosen to discuss the temperature behavior of ΔF^*_{disl}, see below). With $\lambda \sim \xi \sim d \sim 10^{-7}$ cm, $B \sim K/\lambda^2$, the barrier ΔF^*_{disl} can be reduced to the value $\sim 3 \times 10^{-12}$ erg only for fields as high as $H = H_{barrier} \sim 10^4$ kGs, which is two orders of magnitude higher than the value of H_P defined by equation (37) and thus is higher than H_{sat}.

One can argue that the last scenario with single dislocation does not describe correctly the very beginning of the instability and that in fact the transition is preceded by the appearance of the grain boundary composed of a set of circular loops. It means that the layer tilt is large ($\theta \sim 1$ rather than $\theta = d/r_d$) from the very beginning of the instability, but it takes place in the small region with area $\sim \pi r^2$. Unfortunately, this scenario does not improve the situation with the barrier. Really, the elastic energy of the circular grain boundary with small radius r ($r \ll \sqrt{\lambda h}$) is $\sim 2Kr^2/\lambda$ while the diamagnetic energy is $\sim \frac{1}{2}\Delta\chi H^2 \times \pi r^2 \times \frac{2r^2}{\lambda} \sim$

$\pi \Delta\chi H^2 \frac{r^4}{\lambda}$. Extremization of the total energy with respect to r yields an expression for the energetical barrier close to that defined by equation (40) :

$$\Delta F^*_{gb} = \frac{K^2}{\pi\lambda |\Delta\chi| H^2} = \frac{K^{3/2} B^{1/2}}{\pi |\Delta\chi| H^2} . \quad (41)$$

Therefore $\Delta F^*_{gb} \approx \Delta F^*_{disl}$ and the corresponding $H_{barrier}$ remains much higher than H_P. We again come up with the conclusion that the transition cannot occur at $H = H_P$.

There is one important peculiarity in the behavior of ΔF^*_{disl} and ΔF^*_{gb} : both depend on the dilation elastic constant B, in contrast to the analogous quantities ΔF^*_{BN}, ΔF^*_{SN} for the TFCD, which are only K-dependent. Therefore when the temperature T increases towards the SmA-nematic transition, ΔF^*_{disl} and ΔF^*_{gb} diminish because of the decrease of $B = K/\lambda^2$ (K, ξ/λ and d are practically temperature-independent, but λ and ξ grow with T [1, 2]). Recent experiments [32], however, have demonstrated that in fact B *cannot decrease below some limiting value* B_{min}, equal $\sim 10^7$ dyn/cm^2 for typical thermotropic substances such as 8CB or 80CB. Calculations of the lowest values of the ΔF^*_{disl} and ΔF^*_{gb} with $B = B_{min} = 10^7$ dyn/cm^2 show that $\Delta F^*_{disl}/80\, k_B T \sim 1$ and $\Delta F^*_{gb}/80\, k_B T \sim 1$ (i.e. the fluctuation-induced nucleation is possible) starting only with $H_{barrier} \sim 10^3$ kGs. Even in the close vicinity of the phase transitions the barrier height still defines the real threshold of the nucleation of dislocations and, consequently, the expected nucleation of TFCDs induced by these *field-created* dislocations. The situation can be changed only for very thin samples, $h \leq 1$ μm, where in accordance with equation (37) H_P can be as high as 10^3 kGs and thus comparable to or even higher than $H_{barrier}$. Of course, the principal possibility of $B_{min} < 10^7$ dyn/cm^2 and thus $H_{barrier} < H_P$ should not be given up.

The dislocation model gives an additional illustration of the need to consider *two different conditions* for the nucleation of defects [10]. The threshold H_P defined from the condition that the energies of the defect state and initial uniform state are equal, does not guarantee the transition. To initiate the instability, one usually needs higher field $H_{barrier}$ which is able to surmount the barrier of nucleation. The situation is similar to that with TFCDs and is also a direct consequence of the first-order nature of the transition. Thus the idea that the TFCD can nucleate at the *field-induced dislocations* solves the problem only partly : it simply substitutes the problem of ΔF^*_{BN}-barrier by the ΔF^*_{disl}- or ΔF^*_{gb}-barrier problem.

The next principal mechanism is the Helfrich-Hurault instability which is a *second-order transition and thus does not imply the presence of any energy barrier.*

8. Nucleation as a result of the Helfrich-Hurault instability.

Let us consider TFCD creation as a development of the Helfrich-Hurault (HH) instability in a cell with ideally packed SmA layers. This instability is described in terms of a small displacement u along the z-direction which is perpendicular to the unperturbed layers. The lower surface of the cell is assumed to coincide with the x, y plane. The director $\mathbf{n}$ can be expressed in terms of the displacement derivatives $u_i \equiv \partial u/\partial t$ as $\mathbf{n} = (-u_x, -u_y, 1)$. The free energy density f_{HH} associated with the layer displacement can be written in the form [2] :

$$f_{HH} = \frac{1}{2} B u_z^2 + \frac{1}{2} \Delta\chi H^2 (u_x^2 + u_y^2) + \frac{1}{2} K_1 (\Delta_\perp u)^2 + \frac{1}{8} B (u_x^2 + u_y^2)^2 . \quad (42)$$

Here $\Delta_\perp$ is the x, y-part of the Laplace operator.

The HH-perturbation in an ideal sample with perfectly homogeneous surfaces is found [33] to form an infinite rectangular lattice in the sample plane. However, rather single TFCDs

appear in experiments [6-9] which indicates high sensitivity of the domain structure to any irregularity in the cell (dust particle or surface roughness). It is clear that displacement of the layers introduced by inhomogeneities can be so strong that they themselves can cause sufficient decrease of the barrier ΔF^* and thus be an actual cause of TFCD nucleation. Therefore, TFCD nucleation can be attributed to the HH-instability only if irregularity-induced displacements are very small in comparison with that sufficient for nucleation and so are able just to violate the ideal homogeneity of the sample. The first case when the irregularities are strong will be considered as a mechanism of TFCD nucleation in the next section. Here we consider the case when small surface irregularities are able just to initiate local HH-instability and then the formation of the TFCD.

Let us assume that some localized inhomogeneity, whose shape is close to a bump, induces a solitary HH-mode. It is convenient to choose the perturbation in a form of the cylindrical harmonic expansion. In the cylindrical coordinate system (r, φ, z) this expansion has the form

$$u(r, \varphi, z) = \sum_{\ell, m, n} u_0(\ell, m, n)[J_0(q_\ell r) + c_\ell] \sin(knz)(a_m \sin m\varphi + b_m \cos m\varphi), \quad (43)$$

where J_0 is the zero-order Bessel function (J_0 is an eigenfunction of $\Delta_\perp$); c_ℓ, a_m, b_m, $u_0(\ell, m, n)$ are constants; ℓ, m, n are integer. This perturbation must satisfy the following conditions on the upper $(z = h)$ and lower plates $(z = 0)$ and at the domain boundary ∂D:

$$\begin{aligned} u(z = 0) = u(z = h) &= 0, \\ \partial_\perp \mathbf{n}(\partial D) &= 0, \\ u(\partial D) &= 0, \end{aligned} \quad (44)$$

where $\partial_\perp$ denotes the derivative along the direction normal to the boundary ∂D. Substitution of equation (42) in equation (43) and integration over the domain volume makes it clear that the lowest critical field H_{HH} of the HH-effect corresponds to the harmonic with $n = 1$, $m = 0$, which is pure circular. Then the boundary ∂D is a circle $\rho = \rho_{HH} = \text{Cte}$. $\delta_\perp = \frac{1}{\rho}\partial_\rho$ and one can easily obtain from the boundary conditions (44) that $\ell = 1$ and $k = \pi/h \equiv k_{HH}$, $q_1 = \mu_1/R \equiv q_{HH}$, where $\mu_1 = 3.83$ is the first root of the Bessel function $J_1(x)$; $c_1 = -J_0(\mu_1)$.

While layer displacements are determined by the function u, the corresponding stresses caused by them are given by the displacement derivative u_z. The sign of this derivative determines the type of stress: positive u_z corresponds to a compression while negative u_z corresponds to a local decompression or stretching of the layers. The distributions of the displacement u and the stress u_z along the z-axis for the harmonic with $k_{HH} = \pi/h$ are plotted in figures 7a and b (curves 1), respectively. The stress distribution clearly shows that this

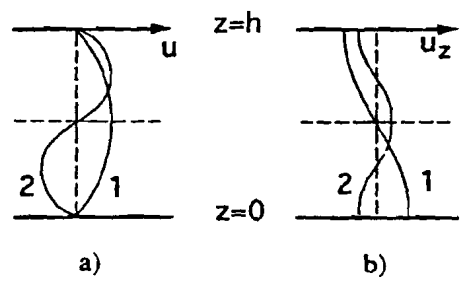

Fig. 7. — Distribution of displacements u (a) and stresses u_z (b) caused in the SmA cell by the first harmonic of the Helfrich-Hurault perturbation (curves 1) and by the second one (curves 2).

harmonic can result only in a surface nucleation of TFCD since it causes displacements with maximum compression at one surface and maximum stretching at the other, and minimum stress at the middle plane of the sample. On the other hand, if the anchoring coefficient $\Delta\sigma$ is sufficiently large, the surface nucleation requires very high free energy. Therefore, if there exists some mode whose stresses correspond to the bulk TFCD nucleation (even if the critical field of such a mode is higher), the nucleation can go this way because bulk nucleation does not depend on $\Delta\sigma$. A mode which is able to cause bulk nucleation turns out to be the harmonic with $\ell = 1$, $m = 0$, $n = 2$ and $k = k_B = 2\,\pi/h = 2\,k_{HH}$. Corresponding displacement ($\sim \sin(2\,\pi z/h)$) and stress distributions are shown in figures 7a and b (curves 2).

For $\ell = 1$, $m = 0$ and arbitrary n the part of the free energy quadratic in u_0 is proportional to $Kq^4 + \Delta\chi\, H^2\, q^2 + Bnk_{HH}^2$, which gives the standard critical field H_{HH} (see [22, 23] and Eq. (20)) and the wave number q_n :

$$\begin{aligned} H_{HH}^2 &= \frac{2\,Knk_{HH}}{\lambda\,|\Delta\chi|} \equiv nH_{HH}^2\,, \\ q_n^2 &= nk_{HH}/\lambda \equiv nq_{HH}^2\,. \end{aligned} \tag{45}$$

Thus, since $k_B = 2\,k_{HH}$, the critical field H_2 of the second harmonic $n = 2$ is $\sqrt{2}$ times larger than that H_{HH} for the first one with $n = 1$.

Now let some field-induced layer displacements take place in the cell. It is natural to assume that the TFCD nucleation occurs when two conditions are satisfied :

(a) the size ρ_0 of the stable TFCD is smaller then the radius $\rho_{HH} = \mu_1/qh$ of the HH perturbation, i.e.,

$$\rho_0 = \frac{\rho_{HH}}{1+\alpha}\,, \tag{46}$$

where ρ_0 is defined as the non-zero solution of the equation $A_1\,\rho + A_2\,\rho^2 + A_3\,\rho^3 = 0$ with coefficients defined by equations (25-30) and $\alpha \geqslant 0$ is some geometrical constant ;

(b) the stress amplitude of the HH-instability exceeds some critical value $u_{z,\max}$ corresponding to the beginning of the dislocation creation, the process which is assumed to be responsible for layer percolation.

We will consider first condition (a) for the first harmonic with $n = 1$, $k = k_{HH}$ which fits the idea of the surface TFCD nucleation. After finding ρ_0 from the equation $A_{SN,1}\,\rho_0 + A_{SN,2}\,\rho_0^2 + A_{SN,3}\,\rho_0^3 = 0$ and substituting it into equation (46), it is not difficult to obtain the critical field

$$H_{a,SN} = \left\{ \frac{12\,\omega_1(1+\alpha)^2}{\mu_1^2} + \frac{1+\alpha}{\mu_1\,\pi^{3/2}} \left[\frac{\Delta\sigma\,\sqrt{\lambda h}}{K} - \omega_2\,\sqrt{\lambda/h} \right] \right\}^{1/2} H_{HH}\,, \tag{47}$$

where H_{HH} is defined by equation (45), $\omega_1 = \beta - 2 - \bar{K}/K$, $\omega_2 = 3 + \beta - \ln\sqrt{2}$. The smallness of the second term within the rectangular brackets, $\lambda/h \sim 10^{-5}$, enables one to simplify the last expression to the form

$$H_{a,SN} = \frac{(1+\alpha)\,\sqrt{12\,\omega_1}}{\mu_1} \left[1 + \frac{\mu_1\,\sqrt{\lambda h}}{12\,\omega_1(1+\alpha)\,\pi^{3/2}} \left(\frac{\Delta\sigma}{K} \right) \right]^{1/2} H_{HH}\,. \tag{48}$$

The critical field $H_{b,SN}$ corresponding to condition (b) can be found by minimizing the total

free energy $\int f_{HH}\, dV$ with f_{HH} given by equation (42), with respect to the perturbation amplitude u_0. It gives

$$H_{b,\,SN} = H_{HH}(1 + \delta^2 h^2)\,, \tag{49}$$

where $\delta = u_{z,\,max}/3\,\pi\lambda$. To be consistent with the u_0-expression (42), one should assume that $\delta^2 h^2 \ll 1$ which takes place for $u_{z,\,max} \ll 20\,\lambda/h$. Thus, if $H_{a,\,SN} > H_{b,\,SN}$, even after the beginning of the process of dislocation creation, the system is waiting for the instant $H = H_{a,\,SN}$ when the perturbations fit the ring nucleation at the surface geometrically. For $H_{a,\,SN} < H_{b,\,SN}$ the scenario is reverse. The free energy of the bulk nucleation ΔF_{BN} is, roughly speaking, two times the surface one ΔF_{SN}, which is negative if the homogeneous state is unstable, meaning that the surface nucleation can not be a final stage of the process. When the surface nucleation due to the development of the first harmonic with $n = 1$ and $k = k_{HH}$ is completed, the ring must go up unless it reaches the middle plane of the sample and thus a bulk TFCD is formed.

As we know, however, if $\Delta\sigma$ is large, the second harmonic with $n = 2$, $k = k_B = 2\,\pi/h$ whose critical field does not depend on $\Delta\sigma$, can cause a direct bulk nucleation. The critical field $H_{a,\,BN}$ of this nucleation can be found by taking $\Delta\sigma = 0$ and H_{HH} to be $\sqrt{2}\,H_{HH}$ in equation (48). It gives

$$H_{a,\,BN} = \frac{2(1+\alpha)\sqrt{6\,\omega_1'}}{\mu_1} H_{HH}\,. \tag{50}$$

The inequality $H_{a,\,BN} \leqslant H_{a,\,SN}$ takes place approximately if the second term in equation (48) is larger than 1, i.e.,

$$\frac{\mu_1\sqrt{\lambda h}}{12(1+\alpha)\,\pi^{3/2}}\left(\frac{\Delta\sigma}{K}\right) > 1\,, \tag{51}$$

which, for our range of parameters, is the case when $\Delta\sigma > 0.6\ \mathrm{erg/cm^2}$.

The principal h-dependence of the critical field of the TFCD nucleation due to the HH-effect coinsides with that of H_{HH}, i.e., $\sim h^{-1/2}$. For sufficiently thick cells, as it follows from equations (48) and (49), the corrections to the $1/\sqrt{h}$ law become important. For example, when the inequality (51) is fulfilled, $H_{a,\,SN}$ does not depend on h for large h. On the other hand, for sufficiently thick samples equation (49) predicts that $H_{b,\,SN}$ increases with h. Finally, the scenario of the undulation-induced nucleation consists in appearance of the undulations when $H = H_{HH}$; then the system waits until the field increases up to the larger value from H_a and H_b, which can produce the TFCD nucleation at the surface or in the bulk [if the inequality (51) is fulfilled]. Both H_a and H_b are expected to be higher than the H_{sat} that defines the growth of the macroscopic domain, as can be clearly demonstrated using figure 6 and one of the conditions of nucleation, for example, equation (46). In accordance with equation (46), the nucleation starts when $\rho_0 \leqslant \sqrt{k/h}$, where $\sqrt{\lambda h}$ is the « size » of the Helfrich-Hurault perturbation in the plane of the cell. This condition is roughly equivalent to $\rho_0 \leqslant 10^{-2}$ for typical cells of thickness $h \sim (10 - 100)\ \mu\mathrm{m}$. As can be seen from figure 6b, $\rho_0 \geqslant 10^{-2}$ and thus the nucleation is achieved only for fields which are much higher than H_{sat}.

The consideration given in sections 7 and 8 corresponds to the *field-driven transitions*. An analogous situation is expected for the strain-induced instability of SmA when the undulations are induced by mechanical stresses [34, 35]. As was observed by Clark and Meyer [35], large displacements of the cell plates produce focal conic domains that presumably are preceded by

periodic undulations. The displacement rate, however, should be fast enough to prevent the reconstruction of the ideal homeotropic structure by moving dislocations.

The Helfrich-Hurault mechanism is neither a unique nor the best way to create TFCD : as we saw, the nucleation field never can be smaller than H_{HH}. There is in principle a possibility to nucleate the TFCD by using essentialy lower fields which are *smaller* than H_{HH} or even smaller than H_{sat}. This possibility is brought about by *bulk dust particles* or by *surface roughness* of the cell plates. It is important to stress that the deformations created by mechanical irregularities are permanent in contrast to those created by the mechanical stresses of the cell with ideally flat plates. Moreover, the mechanism of TFCD nucleation due to irregularities is a general one and explains *both the field-driven and anchoring-driven instabilities.*

9. Nucleation at irregularities.

The main idea of this model is simple : the bulk or surface irregularity distorts the smectic layers and thus the *initial state* is characterized by some nonzero energy due to the B-term in equation (2) ; the nucleation of the TFCD means the *replacement of the dilations by curvature deformations* [the K-term in Eq. (2)], which are generally *less energetic*. The last circumstance should decrease the energy barrier ΔF *. Experimental observations (see [16] and references therein) directly support the scenario of heterogeneous nucleation : it has been revealed that the focal conic domains appear along the dislocation sets rather than in dislocation-free regions.

Let us consider a dust particle with biconical shape of height 2ℓ and radius R, embedded in the matrix of uniform SmA layers (Fig. 8a). The created deformations are relaxed by horizontal

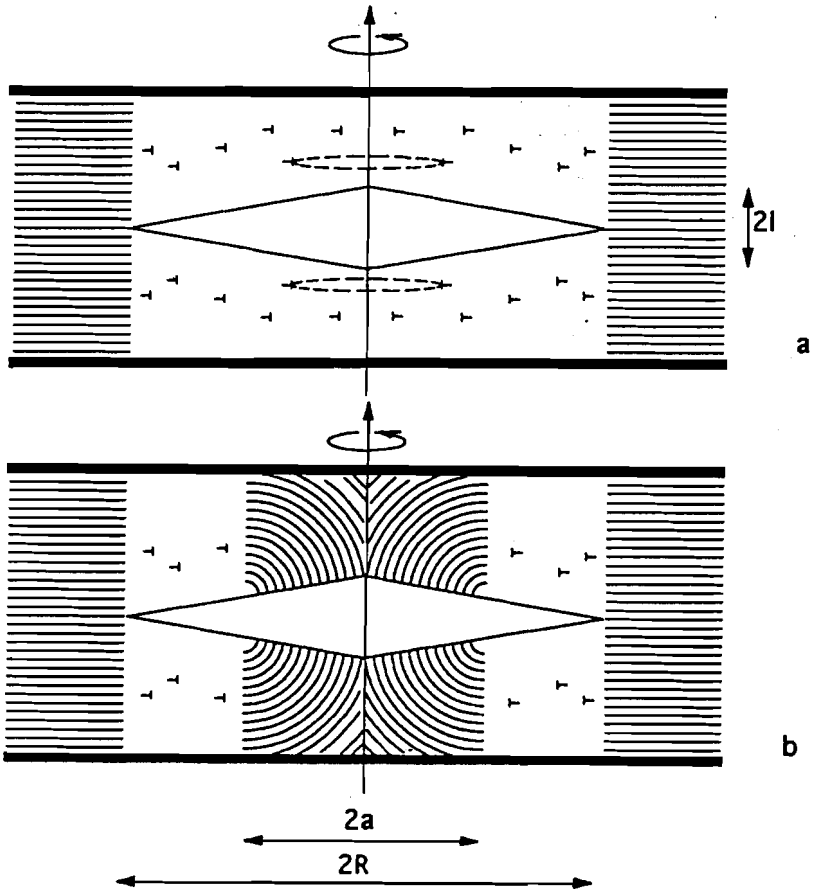

Fig. 8. — Dust particle of biconical shape in the SmA cell : (a) initial state with distortions relaxed by dislocation loops ; (b) nucleation of TFCD.

dislocation loops surrounding the particle. The energy of one dislocation loop with radius r_d is [29, 31] $f_0 = \pi\lambda B d^2 r_d/\xi$, where ξ is a core radius and d is Burgers vector taken equal to one layer thickness. The radii of two successive loops i and $i+1$ are related, $r_{d,i+1} = r_{d,i} + dR/\ell$. Thus the energy of all $n = 2\ell/d$ circular dislocations is

$$F_{\text{disl}} = \pi B d \ell R \frac{\lambda}{\xi} = \pi K \frac{\ell d}{\lambda \xi} R . \tag{52}$$

The last equation does not contain a contribution of the interactions between the loops, i.e., it assumes that the dislocations are independent, which is close to reality when $\ell \ll R$. Also equation (52) does not contain the contribution of strains that are not relaxed by the loops ; these strains are less efficient for the nucleation of TFCD and will be considered later on.

Nonzero elastic energy F_{disl}, which is proportional to R, changes the energy of the initial state. Now instead of equation (8) for the initial state of the volume $\pi a^2 h$, where $a \leqslant R$, one has an expression with a term linear in a :

$$F_0 = \pi K a \ell d/\xi\lambda + 2\pi\sigma_\perp a^2 - \pi \Delta\chi H^2 a^2 (h/2 - \ell/3) ,$$

or, since $\ell \ll h$ and $a = \rho h$,

$$F_0 = (\pi K h \ell d/\xi\lambda)\rho + (2\pi\sigma_\perp h^2 - \pi \Delta\chi H^2 h^3/2)\rho^2 . \tag{53}$$

Now let us consider the TFCD nucleating at the dust particle. The axes of symmetry of the TFCD and the dust particle are supposed to coinside. Within the area occupied at the particle by the TFCD base (now of conical shape) the layers are oriented strictly normal to the particle surface and thus no dislocations are required to fill the space (Fig. 8b). Absence of dislocation in the region occupied by the TFCD means that the surface energy at the interface TFCD/particle can be taken as equal to zero (i.e., we do not consider specific anchoring at the surface of the particle ; however, it is evident that the tangential anchoring of the SmA molecules at the particle would facilitate the nucleation). The biconical shape of the particle allows us to recalculate the energy of the TFCD by simply changing the integration range for the angular parameter θ. The maximal value of θ is defined by the slope ℓ/R of the dust particle surface (Fig. 8b) and thus instead of condition (9) one has

$$\xi \leqslant r \leqslant a/\sin\theta - \xi , \quad \text{arctg}\ (2a/h) \leqslant \theta \leqslant \text{arctg}\ (R/\ell) . \tag{54}$$

The integration of the elastic, diamagnetic, and surface contributions [Eqs. (2), (3) and (5), respectively] using conditions (10) and (54), leads to the new expression for the free energy of the domain formation :

$$\begin{aligned}\Delta F_{\text{BN, disl}} = \Delta F_{\text{BN}} &- (\pi K h \ell d/\xi\lambda)\rho - \\ &- 4\pi K h \rho \left[\left(\ln \frac{h\rho}{\xi} - 2 - \frac{\bar{K}}{K} \right) \text{arcctg}\, \frac{R}{\ell} + L\left(\text{arcctg}\, \frac{R}{\ell} \right) \right] \\ &+ \frac{\pi}{3} \Delta\chi H^2 h^3 \rho^3 \left(\frac{\ell}{R} - \text{arcctg}\, \frac{R}{\ell} \right)\end{aligned} \tag{55}$$

where ΔF_{BN} is defined by equation (17). For $\ell/R \ll 1$ the corrections to the elastic and

diamagnetic contributions are small, of the order of ℓ/R and $(\ell/R)^3$, respectively. It allows us to write the free energy expansion for $\rho \ll 1$ in the form

$$\Delta F_{BN,\,disl} = (A_{BN,\,1} - A_{disl})\,\rho + A_{BN,\,2}\,\rho^2 + A_{BN,\,3}\,\rho^3 + \cdots =$$

$$= 2\,\pi^2 K h' \left(\beta - 2 - \frac{\bar{K}}{K} - \frac{\ell d}{2\,\pi\lambda\,\xi}\right)\rho + 4\,\pi K h(\ln\sqrt{2} - \beta - 3)\,\rho^2$$

$$+ \frac{\pi^2}{6}\Delta\chi\,H^2\,h^3\,\rho^3 + \ldots \qquad (56)$$

The last expression differs from the corresponding free energy for the ideal cell without impurities only by the negative linear contribution $(-A_{disl} = -\ell d/2\,\pi\lambda\,\xi)$ that is brought about by the nonzero dislocation energy of the initial state. The new negative contribution to $\Delta F_{BN,\,disl}$ drastically decreases the height of the energy barrier,

$$\Delta F^{*}_{BN,\,disl} \cong \frac{2(A_{BN,\,1} - A_{disl})^{3/2}}{3\sqrt{3}\,|A_{BN,\,3}|^{1/2}} = \frac{8\,\pi^2 K^{3/2}}{3\sqrt{|\Delta\chi|\,H}}(\beta - 2 - \bar{K}/K - \ell d/2\,\pi\lambda\,\xi)^{3/2}, \qquad (57)$$

and thus increases the possibility of TFCD nucleation. The barrier even completely disappears when $\beta - 2 - \bar{K}/K < \dfrac{\ell d}{2\,\pi\lambda\,\xi}$. With $d \sim \xi \sim \lambda \sim 30$ Å, $\bar{K} = 0$, $\beta \sim 4 - 10$ the last situation is satisfied for particles with height as small as $2\,\ell \gtrsim (20 - 60)\,d$,) i.e. $2\,\ell \sim 10^3$ Å. It simply means that bulk or surface irregularity can nucleate the TFCD even when the external field is absent. Since ξ and λ diverge as one approaches the SmA to nematic transition, the probability of nucleation increases with temperature decrease.

A similar consideration is valid for surface irregularity and the anchoring-driven transition. If the surface irregularity has a conical shape of height ℓ and radius R, the calculation yields for the free energy

$$\Delta F_{SN,\,disl} = (A_{SN,\,1} - A_{disl}/2)\,\rho + A_{SN,\,2}\,\rho^2 + \ldots$$

$$= \pi^2 K h\left(\beta - 2 - \frac{\bar{K}}{K} - \frac{\ell d}{2\,\pi\lambda\,\xi}\right)\rho + \pi K h\left(\frac{\Delta\sigma h}{K} - 3 - \beta + \ln\sqrt{2}\right)\rho^2 + \ldots; \qquad (58)$$

the barrier

$$\Delta F^{*}_{SN,\,disl} \cong \frac{\pi^3 K^2}{4\,|\Delta\sigma|}(\beta - 2 - \bar{K}/K - \ell d/2\,\pi\lambda\,\xi)^2 \qquad (59)$$

is significantly reduced or even completely removed if $\ell \sim 10^3$ Å.

In principle, one can consider also the stress (dislocation-free) mechanism of relaxation around the dust particle. As is well known [1, 2], the disturbance of radius R creates deformations which extend at distances $L = R^2/\lambda \gg R$ along the vertical axis [1, 2]. Let us consider how the stresses caused by the surface conical bump could influence the anchoring-driven TFCD nucleation. The anchoring properties of this bump are the same as those of the flat substrate.

The stress contribution F_{str} to the energy of the initial state can be estimated as the B-term in equation (2). It has different behavior for $R \ll \sqrt{\lambda h}$ and $R \gg \sqrt{\lambda h}$. In the first case the volume of distortions is $\pi R^2 \times (R^2/\lambda)$, and one has from equation (2)

$$F_{str} = \frac{\pi}{2} B\left(\frac{\ell}{h}\right)^2 \frac{R^4}{\lambda} = \frac{\pi}{2} K \frac{\ell^2}{\lambda^3 h^2} R^4. \qquad (60)$$

For $R \gg \sqrt{\lambda h}$ the volume of distortions is restricted by the cell plates and

$$F_{str} = \frac{\pi}{2} B \left(\frac{\ell}{h} \right)^2 hR^2 = \pi K \frac{\ell^2}{2\lambda^2 h} R^2 . \tag{61}$$

As follows from the two last equations, the stress contribution to the free energy of nucleation scales as ρ^4 if $R \ll \sqrt{\lambda h}$ and thus does not change significantly the barrier of nucleation. For $R \gg \sqrt{\lambda h}$ this contribution scales as ρ^2 and the resulting barrier is :

$$\Delta F^*_{SN,\,str} \cong \frac{\pi^3 K^2 (\beta - 2 - \bar{K}/K)^2}{4|\Delta\sigma| + 2\pi K \ell^2/\lambda^2 h} . \tag{62}$$

With the estimates above the desired height of the barrier $\Delta F^*_{SN,\,str} \sim 3 \times 10^{-12}$ erg could be provided by irregularities with amplitude $\ell \sim$ few micrometers. Thus the stress mechanism seems to be less effective than the dislocation one.

The relative importance of the linear and quadratic (or F_{disl} and F_{str}) contributions will depend on the concrete geometry of dust particles or the cell surface and deserves separate consideration. Here it is important just to indicate that the inhomogeneity-nucleated TFCD will expand, « eating » the dislocation loops or strains, up to the point when $a = R$. For $a \gg R$ one should return to the « ideal » case because the matrix outside the domain consists of ideal parallel layers. Thus the TFCD will grow further if $\rho^* h < R$, and will stop if $\rho^* h > R$. The values of ρ^* are defined by equations (32) and (35) for anchoring- and field-induced nucleation, respectively. For the field instability, for example, equation (35) shows that the irregularities with lateral size as small as $R \approx 1$ μm can satisfy condition $\rho^* h < R$ starting with fields ≈ 130 kGs ; this field is smaller than the threshold of the undulation HH-instability (≈ 200 kGs for 100 μm cell [1]). On the other hand, in a real cell there are particular regions where effective R can be much larger than 1 μm : these regions are naturally created by the edges of the smectic sample or by so-called spacers which are used to fix the cell thickness. Thus in real samples we expect the appearance of the TFCDs for fields smaller than H_{HH}.

In conclusion of this section we briefly discuss one additional factor that can help to overcome the barrier ΔF^*_{BN} for small $\rho < 1$ in the particular case of the lyotropic ferrosmectics considered in references [6, 36]. This factor is an intrinsic one connected to the peculiarities of ferrosmectic structure, which can be schematized as a stack of alternating surfactant layers and thin films of ferrofluid [36]. Evidently, the effect of the external field on the structure will be defined exclusively by the coupling with the ferrofluid layers. The pancake-like ferrofluid sheets are unstable in the normal field and will transform into elongated spindles with long axes along the field. The lamellar layers will follow this local transformation (because of finite adhesion), forming a TFCD with the ferrofluid spindle as a core.

10. Conclusion.

We have examined the possible scenarios of the nucleation of focal conic domains in SmA under the action of the surface tension anisotropy or an external field. The consideration is based on the calculation of the energy of the TFCD located in the restricted sample with finite thickness and surface anchoring. The energy of the TFCD is calculated as a function of the domain radius, cell thickness, splay and saddle-splay elastic constants, field strength, as well as the anisotropy in surface energy and permittivity. It is shown that the large-scale and small-scale behaviors of the focal conic domain state are principally different.

For small scales (i.e., focal conic domains with radius smaller that the cell thickness, $\rho = a/h \gg 1$) the expansion of the nucleation energy in a power series of ρ shows that the leading linear term is related to the elastic energy ; the driving forces (anchoring or field) enter only to the quadratic or cubic terms, respectively. Since the elastic energy of the defect is positive, the uniform and defect states are separated by an energy barrier. This barrier is too high to be surmounted by thermal fluctuations for modest values of the field strength or the surface anisotropy. The same problem is shown to be important for the dislocation or grain-boundary model of field effects in the SmA.

To explain numerous experimental observations of the TFCD nucleation we have used an idea that the nucleation is facilitated by local initial deformations of the layers. In principle, these deformations can be brought about either by the Helfrich-Hurault undulations (second-order transition) or by the mechanical inhomogeneities such as dust particles or surface roughness. The first scenario occurs in an ideal cell with highly uniform and flat plates ; its validity is limited by the case of the field-driven effect or fast mechanical stresses. An evident result of this model is that the threshold of the TFCD appearance cannot be smaller than the threshold of the Helfrich-Hurault instability. A more effective and general scenario seems to be the one with bulk or surface inhomogenities. Within the scope of this model, the nucleation of the TFCD replaces compressions by curvature deformations and thus the energy barrier is drastically reduced or even completely removed. With sufficiently large irregularities (of micron size) the nucleation of the focal conic domains can precede other expected instabilities, such as an undulation instability. Sample edges, dust particles, surface irregularities or spacers can serve as natural sources of the domain nucleation.

For large scales ($\rho \gg 1$) the growth of the TFCD is determined by the balance of the surface and field forces. The corresponding « saturation » field H_{sat}, which is able to infinitely increase the size of the domain nuclei, typically turns out to be smaller than the Helfrich-Hurault threshold. It means that in real experiments with perfectly prepared and flat plates a single dust particle or surface irregularity gives rise to the formation of the TFCD which will expand and replace the initial uniform state, if $H > H_{sat}$ (field instability) or $H < H_{sat}$ (surface instability). In the vicinity of the SmA-nematic phase transition the scenario of transitions can be different from that considered above if the dilation elastic constant B significantly decreases ; however, recent experiments [32] show that B remains quite large even in the vicinity of the transition.

The present study requires additional investigations both experimental and theoretical. First, one can suggest special experiments devoted to careful characterization of (a) the distortions caused by dust particles or surface roughness ; (b) anisotropy of the surface energy. These two characteristics should define respectively the appearance and propagation of the TFCDs. Second, we give only a rough estimation of the elastic energy associated with the mechanical irregularities within the scope of continuum theory ; more work should be done on the relationship between the properties of the irregularities and the nucleation energy. Third, our theory is restricted by the TFCD scenario of instability ; it will be interesting to expand this study to other geometries of the domain defects. For example, with negative saddle-splay elastic constant $\bar{K}$ a special type of FCD with positive Gaussian curvature of layers can arise [37, 38]. Another possibility is a formation of parabolic FCDs [39]. Special attention should be paid also to the role of oily streaks, which are in fact the stripe analogs of the focal conics in the layered systems and show specific instabilities under the action of external fields [40, 41]. Recent experiments [18] demonstrate that the stripe domains can significantly change the growth pattern during the described first-order structural transition when $\rho \sim 1$ and the surface anchoring is strong enough (a few erg/cm^2).

Acknowledgements.

We benefited from valuable discussions with P. Fabre, M. Veyssié and C. Quilliet, which initiated this work. The fruitful discussions with A. Chalyi, A. Jákli, P. Palffy-Muhoray, A. Saupe and T. Sluckin are appreciated. We thank E. Landry and A. Mihalus for help with manuscript preparation. The support provided to O.D.L. by the National.Science Foundation under grant DMR89-20147 (ALCOM), by DARPA under contract MDA972-90-C-0037 (NCIPT) and by the Laboratoire de Physique des Solides, Orsay, France, is gratefully acknowledged. Visit of V.M.P. to Southampton had been supported by SERC under grant GR/H70317. The Laboratoire de Physique des Solides and Laboratoire de Minéralogie-Cristallographie are associated with CNRS.

References

[1] de Gennes P. G., The Physics of Liquid Crystals (Clarendon, Oxford, 1974).
[2] Kléman M., Points, Lines and Walls in Liquid Crystals, Magnetic Systems and Various Ordered Media (Wiley, New York, 1983).
[3] Lavrentovich O. D., *Zh. Eksp. Teor. Fiz.* **91** (1986) 1666/*Sov. Phys. JETP* **64** (1986) 984.
[4] Lavrentovich O. D., *Mol. Cryst. Liq. Cryst.* **151** (1987) 417.
[5] Hinov H. P., *Liq. Cryst.* **3** (1988) 1481.
[6] Dabadie J. C., Fabre P., Veyssié M., Cabuil V. and Massart R., *J. Phys. : Condens. Matter.* **2** (1990) SA291.
[7] Fournier J. B. and Durand G., *J. Phys. II France* **1** (1991) 845 ;
Fournier J. B., Warenghem M. and Durand G., *Phys. Rev. E* **47** (1993) 1144.
[8] Jákli A. and Saupe A., *Mol. Cryst. Liq. Cryst.* **222** (1992) 101.
[9] Coates D., Liquid crystal Application and Uses, Chapter 12 : Smectic A LCD-s, B. Bahadur Ed. (World Scientific, New Jersey, 1990) p. 275.
[10] Bodnar V. G., Lavrentovich O. D. and Pergamenshchik V. M., *Zh. Eksp. Teor. Fiz.* **101** (1992) 111/*Sov. Phys. JETP* **74** (1992) 60.
[11] Chou N. J., Depp S. W., Eldrige J. M., Lee M. H., Sprokel G. J., Juliana A. and Brown J., *J. Appl. Phys.* **54** (1983) 1827.
[12] Lavrentovich O. D. and Kléman M., *Phys. Rev. E* **48** (1993) R39.
[13] Kléman M., *J. Phys. France* **38** (1977) 1511.
[14] Steers M., Kléman M. and Williams C. E., *J. Phys. Lett.* **35** (1974) L-21.
[15] Fournier J. B., *Phys. Rev. Lett.* **70** (1993) 1445.
[16] Boltenhagen P., Lavrentovich O. and Kléman M., *J. Phys. II France* **1** (1991) 1233.
[17] Blinov L. M., Kats E. I. and Sonin A. A., *Usp. Fiz. Nauk* **152** (1987) 449/*Sov. Phys. Usp.* **30** (1987) 604 ;
S. Faetti, *Mol. Cryst. Liq. Cryst.* **179** (1990) 217.
[18] Li Z. and Lavrentovich O. D., submitted to *Phys. Rev. Lett.*
[19] Proust J. E. and Perez E., *J. Phys. Lett.* **38** (1977) L-91 ;
Perez E. and Proust J. E., *ibid.*, L-117.
[20] Hinov H. P., *J. Phys. France* **42** (1981) 307.
[21] Gradshteyn I. S., and Ryzhik I. M., Tables of Integrals, Series, and Products (Academic Press, New York, 1980).
[22] Helfrich W., *Appl. Phys. Lett.* **17** (1970) 531.
[23] Hurault J. P., *J. Chem. Phys.* **59** (1973) 2068.
[24] Parodi O., *Solid State Commun.* **11** (1972) 1503.
[25] Porte G., Appell J., Bassereau P. and Marignan J., *J. Phys. II France* **50** (1989) 1335.
[26] Linde A. D., *Nuclear Phys.* **B 216** (1983) 421.

[27] Buzdin A. and Fainberg D., *Phys. Lett.* A **167** (1992) 89.
[28] Boiko V. G., Mogel Kh.-I., Sysoev V. M. and Chalyi A. V., *Usp. Fiz. Nauk* **161** (1991) 77/*Sov. Phys. Usp.* **34** (1991) 141.
[29] Pershan P. S. and Prost J., *J. Appl. Phys.* **46** (1974) 2343.
[30] Friedel J., *J. Phys. Colloq. France* **40** (1979) C3-45.
[31] Kléman M., *J. Phys. France* **36** (1974) 595.
[32] Benzekri M., Claverie T., Marcerou J. P. and Rouillon J. C., *Phys. Rev. Lett.* **68** (1992) 2480.
[33] Dilreau J. M., *J. Chem. Phys.* **60** (1974) 1081.
[34] Delaye M., Ribotta P. and Durand G., *Phys. Lett.* **44A** (1973) 139.
[35] Clark N. and Meyer R. B., *Appl. Phys. Lett.* **22** (1993) 493.
[36] Fabre P., Casagrande C., Veyssié M., Cabuil V. and Massart R., *Phys. Rev. Lett.* **64** (1990) 539.
[37] Bouligand Y., *J. Phys. France* **33** (1972) 525.
[38] Boltenhagen P., Lavrentovich O. and Kléman M., *Phys. Rev. A* **46** R1743 (1992).
[39] Rosenblatt C. S., Pindak R., Clark N. A. and Meyer R. B., *J. Phys. France* **38** (1977) 1105.
[40] Orsay Liquid Crystal Group, *Phys. Lett.* **28A** (1969) 687.
[41] Kléman M. and Friedel G, *J. Phys. Colloq. France* **69** (1969) C4-43.